

Specific luminosity limit of e^+e^- colliding rings

Richard Talman

Laboratory of Elementary-Particle Physics, Cornell University, Ithaca, New York 14853

(Received 25 April 2002; published 7 August 2002)

The luminosity in flat-beam circular colliders is known to “saturate” at some “threshold” beam current above which (because the beam height grows) the luminosity varies (only) linearly with beam current, making both the specific luminosity (luminosity/current) and the beam-beam tune shift parameter ξ_y independent of current. The purpose of this paper is to calculate ξ_y analytically with the goal of maximizing the luminosity. A zero parameter application of the theory to 13 existing storage ring configurations yields theory/experiment equal to 1.26 ± 0.45 for $\xi_{y,\max}$. Parameter values (especially tunes Q_x , Q_y , and Q_s) expected to maximize ξ_y are given. The most favored tune combinations seem not to have been tried so far in colliding beam facilities. The vertical beam growth is ascribed to “parametric pumping” of the vertical betatron amplitude of *each* individual particle by its own (inexorable) horizontal and longitudinal oscillation. A unique determination of the distribution of *all* particles then follows from a *saturation principle* which asserts that *the beam height adjusts itself to the value for which the least stable particle (of probable amplitude) is barely stable*. The difference equation describing the pumping can be solved by numerical iteration or, because it is (almost) linear, it can be solved analytically, at least for amplitudes small enough that resonances remain isolated. Because of the aliasing (or undersampling) characteristic of accelerators, this equation exhibits an even richer spectrum of resonances than the Mathieu equation, which the present theory generalizes. Contrary to the lore of the field (which motivates the intentional increase of damping decrement δ_y using wigglers), the theory presented here predicts the dependence of luminosity on δ_y to be quite *weak*. This is not inconsistent with actual collider performance according to a survey by Rice [D. Rice, Cornell University Report No. CBN 01-09 (2001)] of colliding rings built thus far.

DOI: 10.1103/PhysRevSTAB.5.081001

PACS numbers: 41.75.-i, 29.27.Bd

I. BEAM-BEAM OBSERVATIONS FROM EXISTING e^+e^- STORAGE RINGS

This paper is concerned with “saturation” of the specific luminosity, a phenomenon best understood by referring to experimental data. Luminosity data collected in 1985 by Seeman [1] for a variety of colliding rings (VEPP-2M, DCI, ADONE, SPEAR, CESR, PETRA, and PEP 3B) are shown in Fig. 1. In almost all cases saturation is observed—above some threshold the luminosity increases only linearly with current, and ξ_y (which measures the charge density of the opposing beam in units such that ξ_y is the tune shift caused by passage through the other beam) is correspondingly constant.

This saturation phenomenon is consistent with observation (using synchrotron radiation) of beam shapes. For example, in an early observation at CESR, when the beams were separated, independent of beam current, the beams had rms width 1.4 mm and rms height not greater than 30 μm (diffraction limit of optics); after being brought into collision the widths were sensibly unchanged but the rms beam heights were 58 μm and the beam height then increased proportionally with beam current. This causes the beam-beam tune shift parameter ξ_y to saturate and no longer increase with increasing beam current. The fact that the horizontal profiles are unaffected corresponds to the assumption in this paper that this motion is inex-

orable and the beam height enlargement is ascribed to the parametric pumping of vertical oscillations by horizontal oscillations.

Luminosity behavior of LEP is described by Brandt *et al.* [2]. Saturation of ξ_y is again observed. (There is a suggestion also of saturation of ξ_x in one case. This is mentioned only because, if true, it would contradict a fundamental assumption of the present paper—that the horizontal motion is, except for modest tune shifts to be explained later, independent of beam current.) When running LEP at highest energy, 100 GeV, no saturation was observed up to the highest possible beam current. This would tend to contradict the model being presented except that the authors note that the coupling coefficient could not be reduced below $\kappa = 0.8\%$. According to the present paper, saturation of ξ_y would set in already at arbitrarily small beam current in a perfect ring, but this behavior is masked by any beam height σ_{y0} present due to single beam effects, especially coupling or vertical dispersion. This picture is supported by observed behavior, for example, at CESR and PETRA, in which reducing the coupling reduces the threshold current at which saturation sets in.

In 1983, extrapolating empirically from existing rings to predict future behavior for LEP, Keil and Talman [3] conjectured that the damping decrement $\delta_y = 1/2kf\tau$ (where k is the number of bunches, f is the revolution

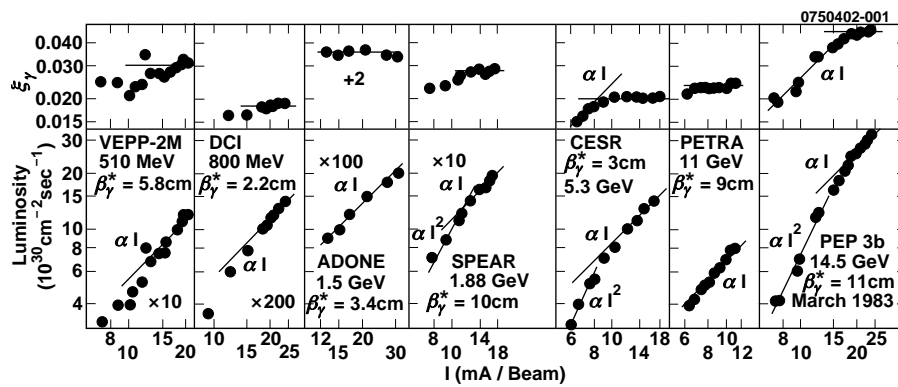


FIG. 1. Tune shift parameter saturation observed (pre-1985) at various e^+e^- colliding beams. Copied from Seeman [1].

frequency, and τ the is damping time) would strongly influence the luminosity saturation behavior. Plotting $\xi_{y,\text{max}}$ against δ_y for rings operating at the time (mainly PETRA and CESR) for values mainly in the range $0.5 \times 10^{-5} < \delta_y < 2 \times 10^{-5}$ a “strong” power law dependence $\xi_{\text{max}} \sim \delta_y^{0.38}$ was found. The luminosity projection for LEP obtained by extrapolating this fit turned out to be almost a factor of 2 too low at lowest energy but roughly correct at higher energies. This suggested a power law exponent considerably smaller than 0.38. Surveying the dependence of ξ_y on δ_y , for numerous modern rings, Rice [4] has produced Fig. 2. This data shows that the power law dependence (to the extent it is applicable at all) could be as weak as $\xi_{\text{max}} \sim \delta_y^{0.05}$.

The present paper attempts to clarify the influence of damping decrement on luminosity, neglecting any multiparticle-coherence aspects. The conclusion (based on theory alone) will be that the dependence is weak.

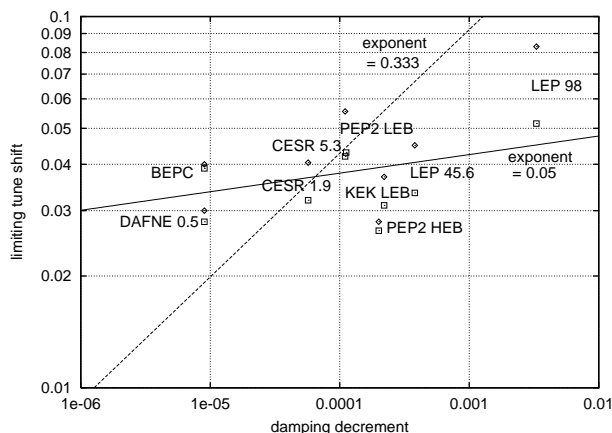


FIG. 2. A survey by Rice of the dependence of beam-beam tune shift parameter ξ_y on damping decrement δ_y , as observed at various, not too ancient, colliding rings. For each ring, determinations of ξ_y by alternative methods are indicated by different symbols. The straight lines represent “weak” ($\xi_y \sim \delta_y^{0.05}$) and “strong” ($\xi_y \sim \delta_y^{0.333}$) power law dependencies.

Beam-beam calculations are often characterized as being weak-strong or strong-strong, depending upon whether or not the opposing beam profile is held fixed. The approach taken here does not really fit either category. On the one hand, the inexorable treatment of horizontal and longitudinal motion of both beams could be characterized as a weak-weak assumption [5]. On the other hand (once the *saturation principle* and the Gaussian profile assumption have been adopted), my treatment of vertical motion can be said to be strong-strong. Another way in which the present calculation differs from earlier calculations is that it includes (essentially) no Monte-Carlo-supplied fluctuations.

Many beam-beam calculations have been reported in the past. By this time fully numerical, strong-strong simulations, in which particles subject to quantum fluctuations are tracked individually in six dimensions, have been reasonably consistent with experimental observations at the various colliding beam facilities. The present calculation is more in the spirit of earlier papers which attempted to distill out essential features. Some of these were primarily numerical [6], others [7] concentrated on analytic treatment of the influence of resonances on large amplitude particles and especially the possibility of diffusionlike growth of particle amplitudes. Nonlinearity provided the unifying thread for these calculations.

This paper, emphasizing, as it does, the near-linearity of the equations describing the process, gives a very different, and far simpler, picture. It is interesting to note one way in which the present model accounts for a feature of an early numerical simulation that seemed mysterious at the time. Paraphrasing Tennyson [8], “When the vertical fluctuations are removed from the mapping (and the damping correspondingly reduced as follows from Tennyson’s Eq. 6) the dependence of beam height on beam current remains essentially unchanged.” From the perspective of this paper, in which the near absence of dependence on vertical damping rate is a central feature, this observation is not surprising. An aspect of Tennyson’s simulation that he found mysterious, and remains mysterious, is a strong dependence of beam height on horizontal fluctuations.

II. QUALITATIVE DESCRIPTION OF THE PARAMETRIC PUMPING MODEL

It is not surprising that the (tiny) beam height is much more sensitive to the beam-beam interaction than is the (large) width. Since the horizontal motion is “hot” and the vertical “cold,” any mechanism that couples these motions tends to affect the vertical motion a great deal, without necessarily affecting the horizontal motion noticeably. The model proposed in this paper accepts this feature without further justification; that is, the horizontal motion of every individual electron is *inexorable*, independent of interaction with the other beam (except for an amplitude-dependent tune shift as the opposing beam currents are increased).

Quite the opposite comments apply to the vertical motion. In an ideal electron storage ring, if there were no cross-plane coupling or other extraneous source of vertical excitation, ξ_y would be infinite because the vertical beam height would be zero [9]. In this ideal limit any ξ_y -dependent instability threshold whatsoever would be exceeded for any finite beam current. In particular, the resonance emphasized in this paper, parametric pumping of vertical oscillations by horizontal oscillations, is certain to occur. (The pumped-parameter here is the vertical betatron tune $Q_y \equiv \mu_y/2\pi$.) In this process, if the threshold is exceeded for any particular electron, the vertical amplitude of this electron will increase up to a well-defined level that depends on ξ_y and a_x , the horizontal amplitude of the particular electron. Furthermore, most of the particles must be under the influence of some such amplitude build up; if some large class (e.g., all particles below one-half sigma horizontal amplitude) were free of perturbation, their vertical amplitudes would damp strongly, again causing unphysically large beam density.

Electrons in one beam do not interact directly with each other, but the result of their simultaneous interaction with all the particles in the other beam is a global equilibrium in which all electrons are at least marginally stable against the parametric pumping. The total effect is that the beam height will have increased to a nonzero value such that ξ_y is just low enough for this marginal stability to be achieved for (essentially) all electrons. The saturation theory (or more properly, saturation principle) now expounded is that *the beam height adjusts itself to the value for which the least stable particle is barely stable* [10]. To turn this principle into a practical theoretical calculation that can predict the vertical beam height it is necessary to qualify the statement slightly by limiting it to particle amplitudes having *appreciable probability*. What is to be calculated is the saturation value of the beam-beam tune shift parameter, ξ_{sat} or, equivalently, the beam height σ_y , which is proportional to $1/\xi_{\text{sat}}$.

Single beam (noncolliding) distributions, both horizontal and vertical, are observed to be Gaussian distributed. This is well understood as being the result of a competi-

tion between quantum fluctuations and damping, both of which are due to synchrotron radiation. It is implicit in assumptions already made that the horizontal distribution is unaffected by the beam-beam interaction. But the parametric pumping, at a minimum, introduces a correlation between horizontal and vertical amplitudes, and is capable, therefore, of causing the vertical distribution to become non-Gaussian. An electron pumped to large vertical amplitude will tend to stay locked on resonance in spite of its damping, for a length of time comparable with the synchrotron radiation equilibration time (typically thousands of turns). On a longer time scale the particles will tend to be knocked off resonance by quantum fluctuation. But, because the parametric pumping growth is (initially) exponential, the amplitude of each particle subject to resonance grows to its limiting value within tens of turns. This paper makes no attempt to analyze the complete dynamic evolution, which is clearly very complicated. Rather *it is assumed that the equilibrium distributions remain Gaussian*, so the entire current dependence of the distribution is encapsulated in the dependence on beam current of a single parameter σ_y .

The leading parametric resonance in mechanical oscillators occurs for drive frequency equal to twice the natural frequency; the result is a response that is a subharmonic of the drive. The theory of this phenomenon has a long history going back at least to Lord Rayleigh [11]. The equation of motion is known as the “Mathieu equation” or, in greater generality, the “Hill equation” [12]. The leading behavior is clearly analyzed by, for example, Landau and Lifshitz [13]. Other than employing difference equations rather than differential equations, the present treatment mirrors the Landau-Lifshitz treatment. The need for difference equations arises because of the impulsive nature of the beam-beam interaction. For the same reason the phenomenon of aliasing, without changing the essence, increases the number of possible resonances and alters the vocabulary. There are striking similarities between Mathieu domains of instability [12] and storage ring domains of instability (see Fig. 11, which is explained in Appendix B). Because the bunch distributions are symmetric horizontally the vertical tune modulation occurs at tune $2Q_x$. Because of the subharmonic nature mentioned earlier in this paragraph, this causes resonance at $Q_y = 2Q_x/2 = Q_x$. Even though this is the same condition as for the so-called “difference resonance” (or “coupling resonance” in accelerator physics jargon) the nature of the resonances are completely different, for example, because the coupling resonance is driven by skew quadrupole forces. Furthermore, parametric resonance is comparably effective for both sum and difference resonances, $Q_x \pm Q_y = \text{integer}$.

Except for detuning at large vertical amplitudes, the equations governing parametric pumping are linear. The detuning can be accounted for using well-established mathematical approximations, for example, as described by Migulin [14].

III. DIFFERENCE EQUATION FOR VERTICAL MOTION

As illustrated in Fig. 3, the vertical deflection of an electron passing through the other beam at a location with lattice function β is [15,16]

$$\begin{aligned} \Delta y' &= -\frac{4\pi\xi}{\beta} \sqrt{\frac{\pi}{2}} \sigma \operatorname{erf}\left(\frac{y}{\sqrt{2}\sigma}\right) \\ &\approx -\frac{4\pi\xi}{\beta} y \left(1 - \frac{y^2}{6\sigma^2}\right), \end{aligned} \quad (1)$$

where the vertical distribution has been assumed to be Gaussian with rms size σ , and the error function dependence results from direct application of Gauss' law assuming $\sigma \ll \sigma_x$. That the appropriate numerical factor has been introduced so that ξ is beam-beam tune shift for a small amplitude particle can be seen: a quadrupole of strength q causes deflection $\Delta y' = qy$ which causes small amplitude tune shift $\Delta Q = -\beta q/4\pi$ [17]. The linear part of the beam-beam deflection is labeled "equivalent quadrupole" in Fig. 3.

To account for the damping that accompanies synchrotron radiation one introduces a small "damping decrement" δ , so that the once-around transfer map in "Twiss form" is

$$\begin{aligned} \begin{pmatrix} y \\ y - \Delta y'/2 \end{pmatrix}_{t+1} &= \exp(-\delta) \begin{pmatrix} C_0 + \alpha S_0 & \beta S_0 \\ \gamma S_0 & C_0 - \alpha S_0 \end{pmatrix} \\ &\times \begin{pmatrix} y' \\ y' + \Delta y'/2 \end{pmatrix}_t, \end{aligned} \quad (2)$$

and a similar equation can be written for backwards propagation from t to $t - 1$. Note that y' is evaluated at the center of the other beam. I am using the notation $C_0 \equiv \cos\mu_0$ and $S_0 \equiv \sin\mu_0$. For these two maps the top equations are

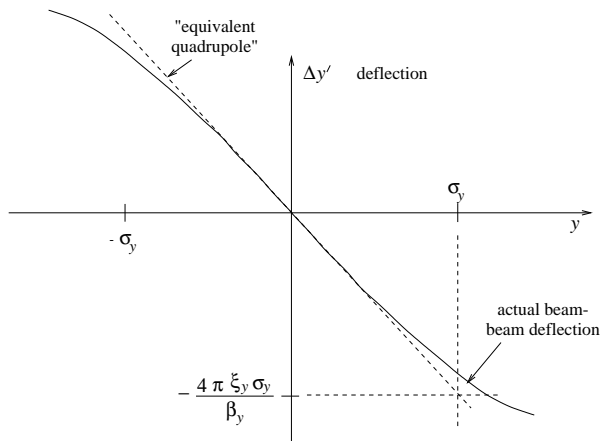


FIG. 3. Dependence of vertical deflection $\Delta y'$ on vertical displacement y . The deflection of an "equivalent" quadrupole of strength $q = -4\pi\xi/\beta$ is also shown. For an e^+e^- collider $\xi > 0$.

$$\exp(+\delta)y_{t+1} = (C_0 + \alpha S_0)y_t + \beta S_0(y' + \Delta y'_t/2), \quad (3)$$

$$\exp(-\delta)y_{t-1} = (C_0 - \alpha S_0)y_t - \beta S_0(y' - \Delta y'_t/2). \quad (4)$$

Treating δ as small and adding these equations to eliminate y' yields [18]

$$y_{t+1} = \frac{2C_0y_t - y_{t-1}(1 - \delta) + \beta S_0\Delta y'_t(x_t, y_t, s_t)}{1 + \delta}. \quad (5)$$

This formula is extremely convenient for *numerically* evolving y into the future by simple iteration; the only substantial calculation required is the determination on each iteration of $\Delta y'_t$ (whose dependence also on transverse coordinate x_t and longitudinal coordinate s_t will be introduced shortly). This evolution can be *stable* or *unstable* in ways to be analyzed. Once $\Delta y'_t$ has been spelled out explicitly, Eq. (5) represents the entire saturation theory— ξ_{sat} is the largest value for which all amplitudes (except those so far out in the tails of the distribution as to be negligible) are stable. This calculation can be performed numerically by checking the stability of Eq. (5) for a sufficiently representative selection of amplitudes and a sufficiently large number of turns.

Within the limitation of the model (for example the uncertainty in picking what constitutes a "probable amplitude" in the saturation principle) the numerical procedure just described can be arbitrarily accurate but, being numerical, it provides little intuitive guidance as to the essence of the process. For such guidance an *analytic* solution of difference Eq. (5) is useful, even if it is quantitatively inaccurate. It is convenient to set $\delta = 0$ for the moment, planning to account for damping later, to approximate the error function according to the final version of Eq. (1), and to move the linear part of the deflection to the left-hand side of the equation. Then the equation of vertical motion is

$$y_{t+1} - 2Cy_t + y_{t-1} = S4\pi\xi \frac{y^2}{6\sigma^2} y. \quad (6)$$

Here we have defined $C \equiv \cos(\mu_0 + 2\pi\xi)$, $S \equiv \sin(\mu_0 + 2\pi\xi)$ in order to incorporate the linear part of the beam-beam deflection into the unperturbed motion. If the right-hand side is evaluated for "zerth approximation" motion $y_t = a_y \cos\mu t$, and only the fundamental Fourier component (varying as $\cos\mu t$) retained, the result is

$$\frac{S\pi\xi}{2} \frac{a_y^2}{\sigma^2} a_y \cos\mu t. \quad (7)$$

Resubstituting $a_y \cos\mu t = y_t$, this term can be incorporated approximately into the equation of motion by defining an amplitude-dependent coefficient [19],

$$\begin{aligned}\bar{C} &= \cos\bar{\mu} = C + \frac{S\pi\xi}{4} \frac{a_y^2}{\sigma^2} \\ &\approx C + \frac{S\pi\xi}{4} \left[1 - \exp\left(-\frac{a_y^2}{\sigma^2}\right) \right].\end{aligned}\quad (8)$$

This transforms the equation of motion into

$$y_{t+1} - 2\bar{C}y_t + y_{t-1} = \beta S \Delta y'_t, \quad (9)$$

where $\Delta y'_t$ is any not-yet-included perturbation. (It is not necessary to replace S by the corrected value \bar{S} since this factor appears only in the perturbing term.) Though \bar{C} will be obtained directly from Eq. (8) when it is needed, the tune at amplitude a can be expressed directly by expanding Eq. (8),

$$\begin{aligned}\bar{\mu} &= \mu_0 + 2\pi\xi \left\{ 1 - \frac{1}{8} \left[1 - \exp\left(-\frac{a^2}{\sigma^2}\right) \right] \right\} \\ &\equiv \mu - \frac{\pi\xi}{4} \left[1 - \exp\left(-\frac{a}{\sigma^2}\right) \right].\end{aligned}\quad (10)$$

The amplitude-dependent part becomes increasingly negative as a increases, which causes the tune shift to be less positive than would be given by the linearized focusing force alone. Until amplitude-dependent detuning becomes an issue there will be no need to distinguish between \bar{C} and C since instability thresholds occur for amplitudes small enough that $\bar{C} \approx C$.

The dependence of horizontal tune on horizontal amplitude will be much the same as that for the vertical motion. The leading variation of $\Delta x'$ is proportional to $1 - x^2/2\sigma_x^2$, just as in Eq. (1).

IV. SUBHARMONIC PARAMETRIC EXCITATION OF VERTICAL OSCILLATIONS

We now turn to the mathematical analysis of beam-beam distortion. From a pedagogical point of view the reader unfamiliar with difference equations might profit from first reading Appendix A, which uses difference equations to solve for betatron response to an external shaker. Because that drive is “direct” the analysis is simpler than this section requires. Higher order parametric resonances are analyzed in Appendix B.

The vertical beam-beam deflection, given previously by Eq. (1), actually depends also on both the horizontal and longitudinal displacements. Because the beams are ribbon shaped, and both profiles are Gaussian, the y -linearized deflection on turn t is given by [20]

$$\begin{aligned}\Delta y'_t &= -\frac{4\pi\xi}{\beta} \exp\left(-\frac{a_x^2 \cos^2 \mu_x t}{2}\right) \\ &\quad \times \sqrt{1 + a_s^2 \left(\frac{\sigma_s}{\beta_y^*}\right)^2 \cos^2 \mu_s t y_t},\end{aligned}\quad (11)$$

where μ_x and μ_s are horizontal and longitudinal tunes (multiplied by 2π) and where units have been chosen so

$\sigma_x = 1$. ξ is now to be interpreted as the value of the tune shift parameter at $x = s = 0$. For much of this paper, in the interest of keeping the formulas simpler, I will concentrate on the transverse motion by taking $a_s = 0$. The same formulas derived for x motion can be easily transcribed to incorporate s when needed. Of course, including another degree of freedom introduces many more resonances. Since $\mu_s \ll \mu_x$ it will be natural to regard the new resonances as “satellites” of the horizontal resonances.

It is appropriate to Fourier expand the Gaussian factor in Eq. (11) [21],

$$\Delta y'_t = -\frac{4\pi\xi}{\beta_y} \left\{ \sum_{n=0}^{\infty} \left[\frac{B_0}{2} + B_n \cos(2n\mu_x t) \right] \right\} y_t. \quad (12)$$

The coefficients B_n can be evaluated in terms of (modified) Bessel functions I_n using an integral from Watson [22], the result is

$$B_n(a_x) = 2 \exp\left(-\frac{a_x^2}{4}\right) I_n\left(\frac{a_x^2}{4}\right). \quad (13)$$

Values of the B_n (which are unrelated to Bernoulli numbers) are given in Table I. The first row and first column are shown only for completeness. B_0 can (and will) be set to zero as far as the mechanism of this paper is concerned. (This is consistent with the formulation described previously, where the leading effect of the beam-beam interaction was defined to be part of the unperturbed motion.) The coefficients $B_n(a_x)$ depend (importantly) on a_x but, for brevity, this argument is suppressed in Eq. (12) and in all subsequent equations.

We hypothesize the response of an individual electron to the parametric drive to be betatron motion for which the dominant part is sinusoidal, with a frequency $\tilde{\mu}$ to be determined,

$$\begin{aligned}y_t &= a \cos[(\mu + \varepsilon_n)t] + b \sin[(\mu + \varepsilon_n)t] \\ &\equiv a \cos\tilde{\mu}t + b \sin\tilde{\mu}t.\end{aligned}\quad (14)$$

Here ε_n , to be defined, is a “small” frequency deviation from the natural frequency. It is possible for any of the terms in the sum (12) to resonate with (and hence cause) this motion. The quantity $\mu + \varepsilon_n$ has been replaced by $\tilde{\mu}$ in Eq. (14) and from here on, even though this suppresses the (essential) index n . The coefficients a and b are “variation of constants” coefficients whose variation will be arranged to satisfy the equation of motion. They are assumed to vary slowly with t ; that is, their fractional changes per revolution are small compared to 1. If they are treated as depending on a continuous variable t , then

$$a_{t\pm 1} \approx a_t \pm \dot{a}_t \quad \text{and} \quad b_{t\pm 1} \approx b_t \pm \dot{b}_t. \quad (15)$$

From this point on, the t subscripts on a and b will be suppressed.

Combining Eq. (12) (with constant term dropped) and Eq. (14) yields

TABLE I. Fourier coefficients $B_n(a_x)$ as given by Eq. (13).

n	$B_n(0)$	$B_n(\sigma_x)$	$B_n(2\sigma_x)$	$B_n(3\sigma_x)$	$B_n(4\sigma_x)$	$B_n(5\sigma_x)$
0	2.0	1.58	0.932	0.575	0.414	0.326
1	0.0	0.196	0.416	0.422	0.358	0.299
2	0.0	0.0122	0.0999	0.199	0.235	0.231
3	0.0	0.000 509	0.0163	0.0680	0.122	0.151
4	0.0	0.000 015 9	0.002 01	0.0180	0.0519	0.0854
5	0.0	0.397×10^{-6}	0.000 200	0.003 90	0.0185	0.0420
6	0.0	0.827×10^{-8}	0.000 016 5	0.000 710	0.005 66	0.0182
7	0.0	0.148×10^{-9}	0.118×10^{-5}	0.000 112	0.001 51	0.007 03
8	0.0	0.231×10^{-11}	0.733×10^{-7}	0.000 015 4	0.000 359	0.002 45

$$\begin{aligned}
-\frac{\Delta y'_t}{4\pi\xi/\beta} &= \sum_{n=1}^{\infty} B_n \cos(2n\mu_x t) [a \cos(\tilde{\mu}t) + b \sin(\tilde{\mu}t)] \\
&= \sum_{n=1}^{\infty} \frac{B_n}{2} \{a \cos[(2n\mu_x - \mu - \varepsilon_n^{(-)})t] - b \sin[(2n\mu_x - \mu - \varepsilon_n^{(-)})t]\} \\
&\quad + \sum_{n=1}^{\infty} \frac{B_n}{2} \{a \cos[(2n\mu_x + \mu + \varepsilon_n^{(+)})t] + b \sin[(2n\mu_x + \mu + \varepsilon_n^{(+)})t]\}. \tag{16}
\end{aligned}$$

Any term in these sums can potentially cause resonance. The frequency offsets $\varepsilon_n^{(\pm)}$ quantify “phase offsets from nearest resonances” by the following relations (for which the overall signs are not significant)

$$\begin{aligned}
2n\mu_x + \mu + \varepsilon_n^{(+)} &= -(\mu + \varepsilon_n^{(+)}) \quad \text{or} \quad \varepsilon_n^{(+)} = n\mu_x + \mu, \\
2n\mu_x - \mu - \varepsilon_n^{(-)} &= +(\mu + \varepsilon_n^{(-)}) \quad \text{or} \quad \varepsilon_n^{(-)} = n\mu_x - \mu. \tag{17}
\end{aligned}$$

Presumably a particular one of these possibilities, for example $n, (-)$, will dominate over all others. From here on the index n will be specialized to indicate this particular dominant case. Then, dropping all other terms, Eq. (16) becomes

$$\Delta y'_t = -\frac{4\pi\xi}{\beta} \frac{B_n}{2} [a \cos(\tilde{\mu}t) - b \sin(\tilde{\mu}t)]. \tag{18}$$

Substitution into Eq. (9) yields

$$\begin{aligned}
y_{t+1} - 2\bar{C}y_t + y_{t-1} \\
= -S2\pi\xi B_n [a \cos(\tilde{\mu}t) - b \sin(\tilde{\mu}t)]. \tag{19}
\end{aligned}$$

(As mentioned earlier, it is initially unnecessary to distinguish between \bar{C} and C .) Including the time variation of a and b , Eq. (14) yields

$$\begin{aligned}
y_{t+1} &= (a + \dot{a}) [\cos\tilde{\mu} \cos(\tilde{\mu}t) - \sin\tilde{\mu} \sin(\tilde{\mu}t)] \\
&\quad + (b + \dot{b}) [\sin\tilde{\mu} \cos(\tilde{\mu}t) + \cos\tilde{\mu} \sin(\tilde{\mu}t)], \\
y_{t-1} &= (a - \dot{a}) [\cos\tilde{\mu} \cos(\tilde{\mu}t) + \sin\tilde{\mu} \sin(\tilde{\mu}t)] \\
&\quad + (b - \dot{b}) [-\sin\tilde{\mu} \cos(\tilde{\mu}t) + \cos\tilde{\mu} \sin(\tilde{\mu}t)]. \tag{20}
\end{aligned}$$

Substituting into Eq. (19), and requiring the sine and cosine term coefficients to vanish separately, yields the equations

$$\begin{aligned}
-\dot{a} \sin\tilde{\mu} + b \cos\tilde{\mu} - \bar{C}b - S\pi\xi B_n b &= 0, \\
\dot{b} \sin\tilde{\mu} + a \cos\tilde{\mu} - \bar{C}a + S\pi\xi B_n a &= 0. \tag{21}
\end{aligned}$$

Seeking a solution for which a and b exhibit time dependence of the form $\exp(i\omega t)$ yields

$$\begin{pmatrix} -i\omega & \frac{\cos\tilde{\mu} - \bar{C} - S\pi\xi B_n}{\sin\tilde{\mu}} \\ \frac{-\cos\tilde{\mu} + \bar{C} - S\pi\xi B_n}{\sin\tilde{\mu}} a & -i\omega \end{pmatrix} \begin{pmatrix} a \\ b \end{pmatrix} = 0. \tag{22}$$

The requirement for a nontrivial solution to exist is that the determinant formed from the coefficients must vanish; this yields

$$\omega^2 = \frac{(\cos\tilde{\mu} - \bar{C})^2 - (S\pi\xi B_n)^2}{\sin^2\tilde{\mu}}. \tag{23}$$

In this form the condition for *stable* motion is that ω^2 be *positive* (since the alternative yields one exponentially growing solution). Making the assumptions $\varepsilon_n \ll 1$ and $C = \bar{C}$ allows the approximations $\cos\tilde{\mu} - \bar{C} \approx -S\varepsilon$, $\sin\tilde{\mu} \approx S$. Then setting $\omega = 0$ to determine the edges of a “stop band” yields [23]

$$\varepsilon^2 = (\pi\xi B_n)^2 \quad \text{or} \quad -\pi\xi B_n < \varepsilon < \pi\xi B_n. \tag{24}$$

By setting δ to zero we have so far been neglecting damping and have found that, even with no damping, if ε lies outside the stop band, the motion will be stable. In fact there *is* damping, as represented by $\delta \neq 0$. The threshold of instability is therefore determined by requiring the growth rate given by Eq. (23) to be equal to δ ,

$$\sqrt{-\varepsilon^2 + \pi^2 \xi^2 B_n^2} = \delta. \quad (25)$$

The band of instability is therefore given by

$$-\varepsilon_l < \varepsilon < \varepsilon_l, \quad \text{where } \varepsilon_l = \sqrt{\pi^2 \xi^2 B_n^2 - \delta^2}. \quad (26)$$

For $\delta > \pi \xi B_n$ there is no unstable band at all. It is in this resonance-suppressing role that δ might be expected to have its greatest potential influence on luminosity.

The prediction so far is that the motion is either stable or that, within a limited band, the amplitude grows exponentially without limit. Such growth would eventually invalidate the small amplitude assumption on which the equation is based and, in fact, the amplitude-dependent detuning analyzed earlier limits the growth. Because of the nonlinearity, as well as the state of equilibrium with $a_y^2 = 0$, there is a state of equilibrium with $a_y^2 = a^2 + b^2 \neq 0$. Substituting for \bar{C} from Eq. (8), Eq. (23) depends on the amplitude parameter a_y . After rearrangement the condition becomes

$$\begin{aligned} \varepsilon &= \pm \sqrt{\pi^2 B_n^2 \xi^2 - \delta^2} - \frac{\pi \xi}{4} \left[1 - \exp\left(-\frac{a^2 + b^2}{\sigma^2}\right) \right] \\ &\approx \pm \sqrt{\pi^2 B_n^2 \xi^2 - \delta^2} - \frac{\pi \xi}{4} \frac{a_y^2}{\sigma^2}. \end{aligned} \quad (27)$$

If there is an unstable band then $\pi^2 B_n^2 \xi^2 - \delta^2$ is positive so picking the positive-sign square root yields a positive value for a^2 throughout the stop band of Eq. (26). This equation sets the amplitude at which the growth of vertical amplitude is limited by the amplitude-dependent detuning. The vertical amplitude of any particle whose tunes place it in the range Eq. (26) will be pumped immediately to the value given by Eq. (27). The functions of Eq. (27) are plotted schematically in Fig. 4. It can be seen that stable motion with $a \neq 0$ is even possible for $\varepsilon < -\varepsilon_l$. This asymmetry in ε will be important in interpreting numerical solutions of the master difference equation. In particular, it

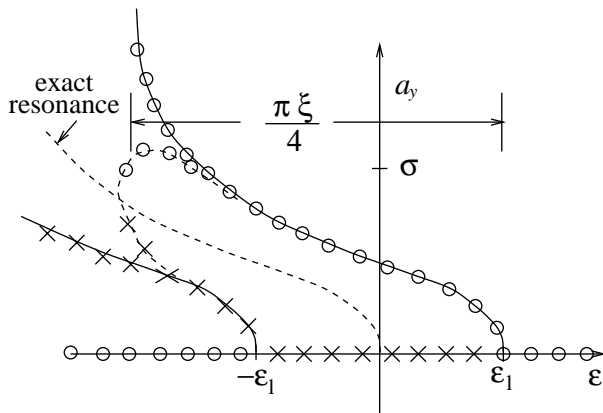


FIG. 4. Plot of Eq. (27). Open circles mark stable motion: a temporary excursion to larger a_y moves the system away from exact resonance which tends to reduce a_y . Crosses mark unstable motion. The broken curve indicates the type of dependence to be expected from a more detailed theory including other nonlinearity.

seems to account for the numerically observed superiority of values Q_x just above resonance compared to values just below.

For the special case $\delta = 0$ the band limits are at $\varepsilon = \pm \pi \xi B_n$ so the amplitude lies in the range $0 < a_y < \sim 2\sqrt{2B_n} \sigma$. From Table I one notes that values of B_n likely to be important vary over the range from, for example, 0.05 to 0.5, depending on a_x , so the limiting amplitude ranges from close to zero up to about 2σ . As the particle oscillates its loss of vertical amplitude due to radiation damping will tend to be replenished immediately by the pumping mechanism and the particle will oscillate rather stably for many turns. But the particle's random walk in horizontal phase space will eventually disrupt the resonance. Positive damping ($\delta > 0$) reduces the limiting amplitude (though typically very little) and, as noted previously, reduces the stop band width.

There is a certain self-consistency here—whatever the beam height is, at least approximately, the pumping mechanism provides the support for just that beam height. This “natural” relationship corroborates the identification of detuning as the amplitude-establishing mechanism since the height scale on which detuning occurs is about the same as the beam height itself. Just what this height σ is remains to be determined. The further relation that, in principle, fixes σ is that ξ depends inversely on σ . The relation can be written as

$$\xi = \frac{I'}{\sigma}, \quad (28)$$

where I' is the beam current, as measured in units chosen to make the constant of proportionality be 1. The factors entering this relation are all well known in practice.

Though it is still too encumbered with limitations to give an accurate picture, and it is not clear what form of averaging is appropriate, Eq. (27) can be manipulated to express this self-consistency semiquantitatively. Since the beam height is supposed to be ascribable to the pumping mechanism that the equation describes, one has to suppose $a \approx \sigma$ is typical. With this assumption Eq. (27) determines ξ according to

$$\begin{aligned} \frac{1}{2} \xi^2 - \frac{\varepsilon}{4\pi B_n^2} \xi - \frac{\varepsilon^2 + \delta^2}{2\pi^2 B_n^2} \approx 0, \\ \text{assuming } 16B_n^2 \gg 1, \end{aligned} \quad (29)$$

which can be solved to give

$$\xi_{\max} \approx \frac{1}{\sqrt{2}\pi B_n} \left(\frac{\varepsilon}{2\sqrt{2} B_n} + \sqrt{\varepsilon^2 + \delta^2} \right). \quad (30)$$

Then σ is determined by Eq. (28). To be valid at all this formula assumes that a single resonance is dominant and that ε corresponds to that resonance. The structure of this formula predicts that the dependence of ξ_{\max} on δ is more complicated than the power law dependence mentioned earlier. In any case the main purpose of Eq. (30) is to illustrate an in-principle, parameter-free, determination of

the limiting tune shift parameter. Since $\delta \ll \epsilon$ is typical, Eq. (30) exhibits only a very weak dependence on δ . This contrasts with the threshold tune shift value which, according to Eq. (39), depends sensitively on δ .

V. OTHER RESONANCES

Equation (14) was not the most general possibility for parametric resonance. For example, suppressing the t subscripts (as before) to free up a position for Fourier indices, let us seek a solution of the form

$$y = a_0 + \sum_{m=1}^3 a_m \cos(m\tilde{\mu}_y t) + \sum_{m=1}^3 b_m \sin(m\tilde{\mu}_y t), \quad (31)$$

truncated, in this case, at $m = 3$.

Performing the same substitutions as before leads to definitions, such as those in Eq. (17), that pick out tune combinations for which the perturbed frequency matches the fundamental frequency. Recalling that $\mu_y + \epsilon_n \equiv \tilde{\mu}_y$,

$$2n\mu_x - (s+1)\tilde{\mu}_y = \tilde{\mu}_y \quad \text{or} \quad 2n\mu_x = (2+s)\tilde{\mu}_y, \quad (32)$$

where s is another integer. The case $s = 0$ was previously called ‘‘lowest order.’’ Let us try $s = -1$, so $2n\mu_x = \tilde{\mu}_y$, or $\epsilon_n = 2n\mu_x - \mu_y$. Solving the resulting equations yields

$$a_2 = \frac{S_y \pi \xi_y B_n}{C_y - \cos 2\tilde{\mu}_y} a_1, \quad b_2 = \frac{S_y \pi \xi_y B_n}{C_y - \cos 2\tilde{\mu}_y} b_1. \quad (33)$$

The stop band edges are unbalanced:

$$\epsilon_{n1} = -\frac{S_y (\pi \xi_y B_n)^2}{C_y - \cos 2\tilde{\mu}_y}, \quad (34)$$

$$\epsilon_{n2} = S_y (\pi \xi_y B_n)^2 \left(\frac{2}{1 - C_y} + \frac{1}{C_y - \cos 2\tilde{\mu}_y} \right).$$

This resonance, with $n = 1, s = -1$, is not really ‘‘new’’ since it requires the same relation between Q_x and Q_y as the lowest order resonance with $n = 2, s = 0$, but the numerical factor and resonant denominators are different. Compared to the limit given in Eq. (24) these acquire factors of order $\pi \xi_y B_n$. Referring to values of B_n given in Table I, and expecting the factor $\pi \xi_y$ to not exceed, for example, 0.3, the only values of n likely to be significant will not exceed a few unless one of the denominators is anomalously small. Several parametric resonances are therefore candidates to dominate the growth of the vertical beam size, even without including longitudinal oscillations.

To incorporate damping decrement δ_y , one should first solve the determinant equation for the growth rate. This should then be set equal to the δ_y to find the stability limits in the presence of damping, as in Eq. (25). It is simpler to mimic Eq. (26) by interpreting ϵ_{n1}^2 as the square of a real frequency shift and to equate it to δ_y^2 , which is the

(negative) square of an imaginary frequency shift. (Doing the same with ϵ_{n2}^2 will not yield quite the same value. This reflects the fact that the threshold of instability need not occur at exactly $\epsilon = 0$.) The first estimate yields

$$\xi_y = \frac{\delta_y^{1/2}}{\pi B_n} \sqrt{\frac{C_y - \cos 2\tilde{\mu}_y}{\sin \tilde{\mu}_y}}. \quad (35)$$

Another resonance occurs for $s = 1$, i.e., for tunes satisfying $2n\mu_x = 3(\mu_y + \epsilon_n)$ or $\epsilon_n = (2/3)n\mu_x - \mu_y$. Solving the resulting equations, both stop band limits are given by

$$\epsilon_n = S_y (\pi \xi_y B_n)^2 \left(\frac{1}{\cos 2\tilde{\mu}_y - C_y} \right). \quad (36)$$

The implication of equality of these limits is presumably that the stop band width is of higher order in ξ than has been used in the calculation. This probably makes this resonance unimportant and accounts for the absence of $s = 1$ stop band in Fig. 11.

It is tedious to extend this calculation to higher order. In Appendix B this extension is made more systematic by using complex exponentials.

VI. IMPORTANT RESONANCES AND FAVORED REGIONS

The master formula governing exact resonance is Eq. (B7). Expressed in terms of tunes it is

$$Q = \pm \frac{2n}{2+s} Q_x, \quad (37)$$

where n is a positive integer and s is any integer except -2 . The aliasing is such that multiples of $1/2$ can be added (or subtracted) from either Q_x or Q . The leading possibilities are tabulated in Table II.

As usual the resonances can be identified with straight lines in a resonance diagram such as Fig. 5. The aliasing can be implemented using ‘‘periodic boundary conditions.’’ When a line terminates on an integer boundary, another line with the same slope starts from the same location on the opposite boundary.

The essential feature of the parametric growth mechanism that has been analyzed is that there is stability up to a threshold above which the amplitude grows rapidly to an amplitude limited by detuning. The stop band widths increase with increasing ξ_y and they are also expanded by the spread of horizontal tunes. There is also a spread of vertical tunes, but this mainly leads to detuning that has to be modeled explicitly, as has been discussed; this effect is automatically included in the numerical investigation described in the next section.

The single resonance model assumes that it is impossible to avoid all resonances and that, for any given operating conditions, it is necessary only to identify and analyze the dominant resonance. In this case the onset of beam growth is controlled by δ . For the lowest order ($s = 0$) resonance, according to Eq. (26), the instability sets in at

TABLE II. The leading linear parametric resonances, including aliases. These resonance lines are plotted in Fig. 5.

n	s	$\frac{2n}{2+s}Q_x$	Aliases	$-\frac{2n}{2+s}Q_x$	Aliases
1	0	Q_x	+0.5, +0, -0.5	$-Q_x$	+1.5, +1, +1.5
2	0	$2Q_x$	+0.5, +0, -0.5, -1, -1.5	$-2Q_x$	+2.5, +2, +1.5, +1, +0.5
1	-1	$2Q_x$	+0.5, +0, -0.5, -1, -1.5	$-2Q_x$	+2.5, +2, +1.5, +1, +0.5
1	1	$2Q_x/3$	suppressed (Fig. 11)	$-2Q_x/3$	suppressed

$$\xi_{n,0} = \frac{\delta}{\pi B_n}, \quad (38)$$

where the second subscript stands for $s = 0$. This is a special case of formulas for ξ_{sat} derived in Appendix B which take the form

$$\xi_{n,s} = \frac{1}{\pi B_n} \delta^{1/(1+|s|)} T_{n,s}^{1/(1+|s|)}, \quad (39)$$

where $T_{n,s}$ is a trigonometric function of the tunes, whose value is approximately 1. For example, from Eq. (35)

$$\xi_{n,-1} = \frac{\delta^{1/2}}{\pi B_n} \sqrt{\frac{C_y - \cos 2\tilde{\mu}}{S_y}}. \quad (40)$$

For this resonance the power law exponent is 0.5.

Tune combinations that approximately satisfy the $s = 0$ resonance condition yield such small values of $\xi_{y,\text{thr}}$ that it seems reasonable to suppose they have always been, and will always be, avoided operationally. One might say therefore that for “unfavorable” tunes the power law exponent is ~ 1 since $\xi_{y,\text{thr}} \sim \delta_y$. For “once-removed” resonances, $s = \pm 1$, $\xi_{y,\text{thr}} \sim \sqrt{\delta_y}$ and the power law exponent is 0.5.

The single resonance model may give a good description in regions where a single resonance is dominant, but in these regions the saturation threshold is necessarily very

low. Such regions are avoided in practice since the goal of colliding beams is high luminosity and there is too much operational overhead to spend machine studies time investigating unpromising tune combinations. As a result there tends to be little data with which to test the single resonance model. In practice the tunes are adjusted to be roughly equidistant from the two or three nearest resonances, invalidating the single-resonance assumption. The numerical approach, to be described next, automatically includes the effects of overlapping resonances.

VII. SOLUTION OF THE DIFFERENCE EQUATION BY NUMERICAL ITERATION

The analytic solution given thus far breaks down when the particle amplitude increases to a value such that more than one resonance is significant. Then a numerical approach is required. The difference equation (5) and deflection formula (1) can be combined into a formula that makes turn-by-turn iteration easy,

$$y_{t+1} = \frac{1}{1 + \delta} \left\{ 2C_0 y_t - y_{t-1}(1 - \delta) - 4\pi \xi S_0 \right. \\ \times \exp\left[\frac{-a_x^2 \cos^2[\mu_x(a_x)(t + t_x)]}{2} \right] \\ \times \sqrt{1 + \left(\frac{\sigma_s}{\beta_y^*}\right)^2 a_s^2 \cos^2[\mu_s(t + t_s)t]} \\ \left. \times \sqrt{\frac{\pi}{2}} \operatorname{erf}\left(\frac{y_t}{\sqrt{2}}\right) \right\}. \quad (41)$$

After substituting for $\mu_x(a_x)$ from Eq. (10), this formula is completely explicit [24]. Since Eq. (41) gives the correct dependence of $\Delta y'$ on y it includes effects nonlinear in y , such as island overlap and chaos, but this paper concentrates on small amplitudes where such effects are expected to be unimportant.

My procedure in using Eq. (41) has been to fix Q_x , Q_y , a_x , and a_s and to increase ξ in steps until instability occurs. Note that, for some small enough amplitude, for example $y_{\min} = 0.001\sigma$, the equation is essentially linear and the motion is stable—the Courant-Snyder (CS) invariant of the motion even decays because $\delta > 0$. Furthermore, Eq. (41) is *pseudohomogeneous* in the sense that $y_t = 0$ for all time is a solution, no matter how large ξ . This makes it necessary to assign a small starting seed amplitude y_{\min} , which may or may not grow due to parametric pumping. The “instability boundary” is defined as

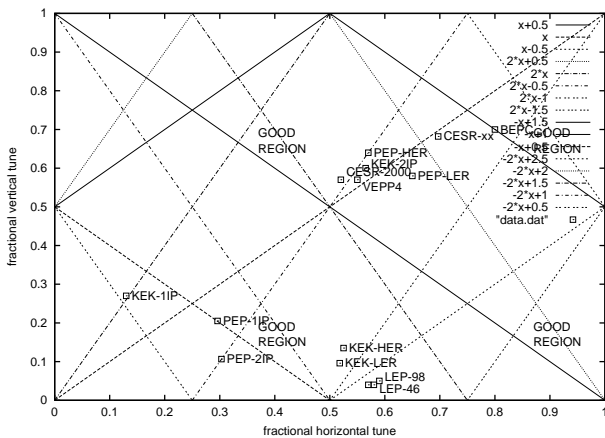


FIG. 5. Linear parametric beam-beam resonances from Table II. In all cases tunes are fractional tune advances (i.e., deviations from nearest lower integer) per IP. None of the operating points are even close to regions labeled “Good Region” on the basis of the *saturation principle*, numerically investigated.

follows: as ξ is increased from zero, a smallest value ξ_{\min} is found for which $y_t > y_{\max}$ for some value of t within a “large” number of turns, for example $N_t = 1000$; here, for example, $y_{\max} = 0.1\sigma$ is an assigned “large” amplitude. [To partially suppress possible artificial correlations among Q , Q_x , and Q_y the parametric drive oscillations were given random starting t indices in the range from 0 to -100 . This is indicated by t_x and t_s in Eq. (41).] The value ξ determined in this manner will be called ξ_{sat} to distinguish it from the differently calculated, single-resonance threshold ξ_{thr} . For most studies the definition of what constitutes probable amplitudes was taken to be the nine combinations of the points $a_x = 0.5\sigma_x, 1.5\sigma_x, 2.5\sigma_x$ and $a_s = 0.5\sigma_s, 1.5\sigma_s, 2.5\sigma_s$. Bringing this up to 16 combinations by including $a_x = 3.5\sigma_x$ and $a_s = 3.5\sigma_s$ did not change the results markedly.

The procedure just described was performed for all points in the transverse tune plane, in steps of 0.01, for various choices of the other parameters. Results are shown in the following series of figures. Figure 6 shows results with synchrotron oscillations absent (i.e., $a_s = 0$) for $\delta = 10^{-4}$. The starting and instability-defining amplitudes here were $(y_{\min}, y_{\max}) = (0.001\sigma_y, 0.1\sigma_y)$; that is, instability was defined to mean parametric pumping from $\sigma_y/1000$ to $\sigma_y/10$. (Though the blowup factor is large, the blown-up amplitude is relatively small.) In this and the other gray scale figures the horizontal

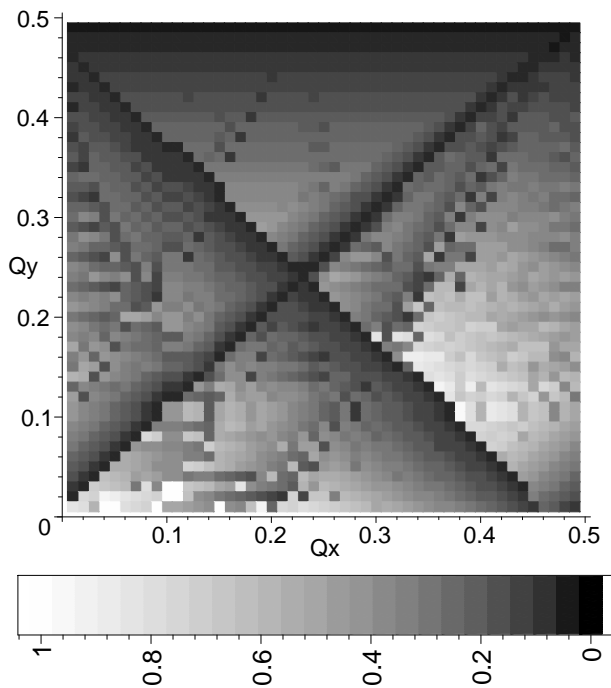


FIG. 6. $a_s = 0$, $\delta = 10^{-4}$. For all points in one quadrant of the fractional Q_x, Q_y tune plane the minimum value of $\xi_{\text{sat}}(a_x)$, for a representative sample of a_x values, has been selected and plotted. In this and other gray scale plots the numerical value of ξ_{sat} is to be obtained using the gray scale to read the factor by which the maximum (pure white) value (in this case $\xi_{\text{max}} = 0.3$) is to be multiplied to obtain $\xi_{\text{sat}}(a_x)$.

amplitude choices were $a_x = 0.5\sigma_x, a_x = 1.5\sigma_x$, and $a_x = 2.5\sigma_x$. At each point the worst case is plotted. By the *saturation principle* this gives the tune plane dependence of ξ_{sat} . In this case synchrotron oscillations are assumed to be absent. The most favorable region seems to be in the vicinity of $(Q_x, Q_y) = (0.40, 0.17)$ where $\xi_{\text{sat}} = 0.19$. Using the four quadrant symmetry

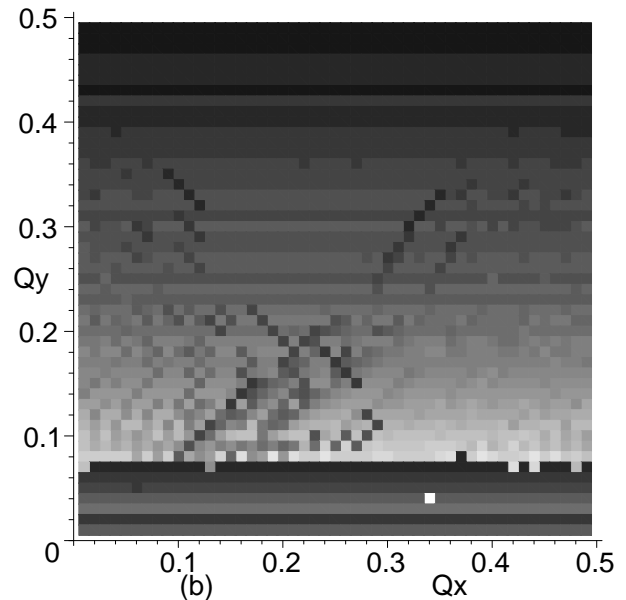
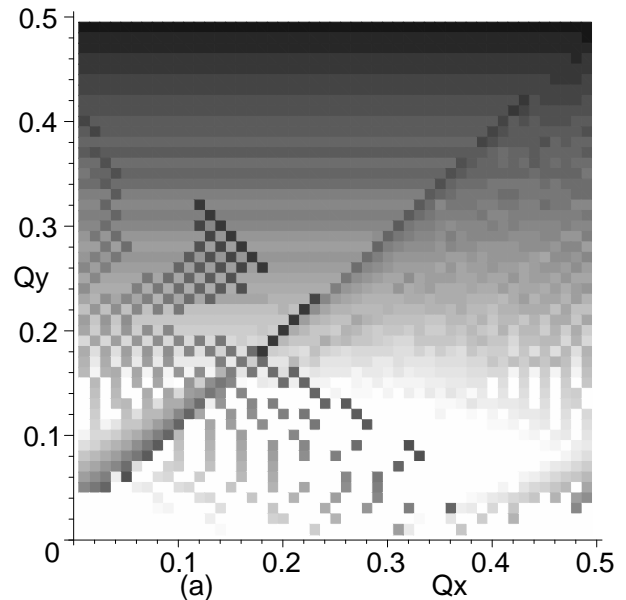


FIG. 7. (a) $a_s = 0.5$, $\xi_{\text{max}} = 0.3$, (b) $a_s = 2.5$, $\xi_{\text{max}} = 0.3$. For both figures $a_x = 0.5$, $\delta = 10^{-4}$. The tune plane dependence of ξ_{sat} is shown for a_s increasing from bottom to top. (Figure 8 differs only by having $a_x = 2.5$.) The gray scale in Fig. 6 is to be used to extract numerical values, with ξ_{max} being pure white. According to the *saturation principle*, the maximum specific luminosity at each point in the tune plane is obtained by picking the lowest value from a sufficiently comprehensive grid of data sets such as these.

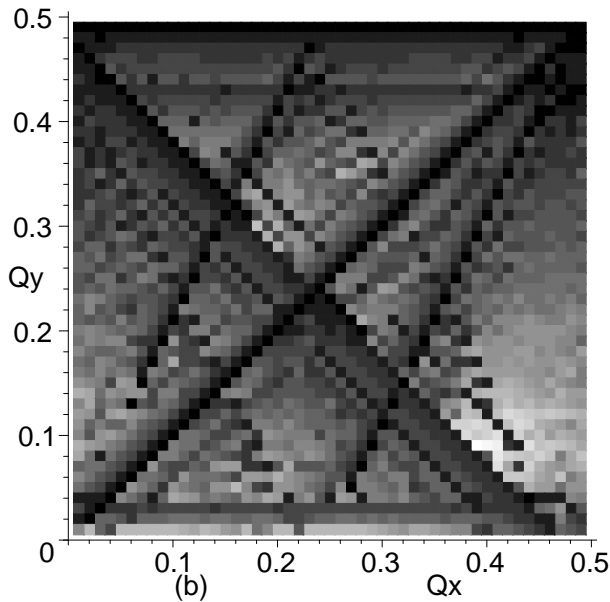
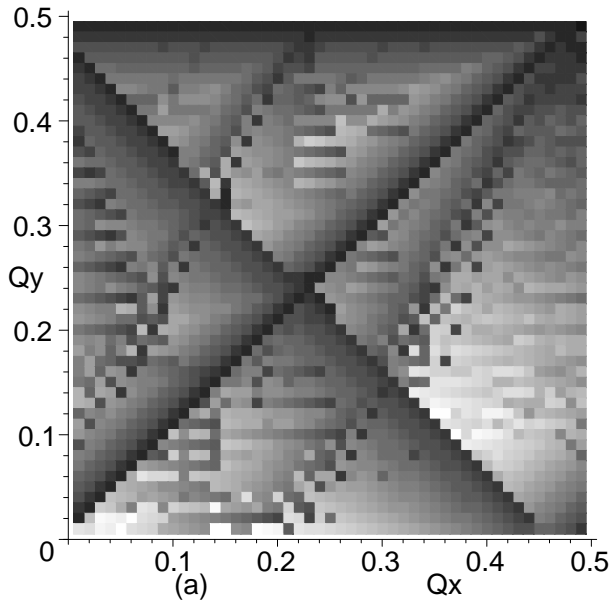


FIG. 8. (a) $a_s = 0.5$, $\xi_{\max} = 0.3$, (b) $a_s = 2.5$, $\xi_{\max} = 0.23$. For both figures $a_x = 2.5$, $\delta = 10^{-4}$. The relationship of these figures to those in Fig. 7 is explained in the caption to Fig. 7. Note that the ξ_{\max} values in (a) and (b) are different. The systematically superior performance on the more positive Q_x side of resonances is ascribed in Sec. IV to the response illustrated in Fig. 4.

plane, equivalent examples are $(Q_x, Q_y) = (0.40, 0.67)$, $(0.90, 0.17)$, and $(0.90, 0.67)$.

The effect of the simultaneous presence of horizontal and longitudinal oscillation is shown in Figs. 7 and 8, again for the case $\delta = 10^{-4}$. The synchrotron amplitude a_s increases by $2\sigma_s$ from bottom to top, and the horizontal amplitude a_x increases by $2\sigma_x$ in going from Fig. 7 to Fig. 8. The worst case values from these

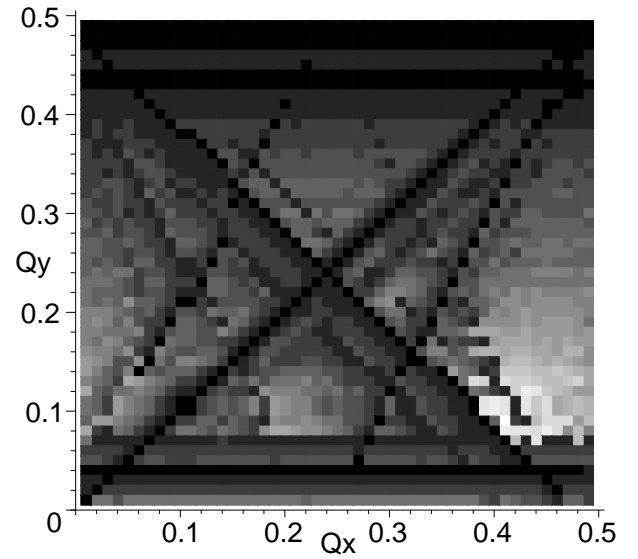


FIG. 9. $\delta = 0.0001$, $\xi_{\max} = 0.190$. At each point in the tune plane the worst case from a complete grid of data sets such as those in Figs. 7 and 8 (combined) is picked and plotted, in this case with *weak* damping.

plots have been selected and plotted in Fig. 9. Figure 10 is obtained similarly, but with $\delta = 10^{-2}$. The presence of just those resonances predicted by the model (Table II) is clear. Note the close similarity of Figs. 9 and 10, and therefore the comparatively weak dependence on δ . Apart from the modest increase of ξ_{\max} from 0.19 to 0.20, and a slightly brighter region in the lower right hand corner with $\delta = 10^{-2}$, the plots are qualitatively similar.

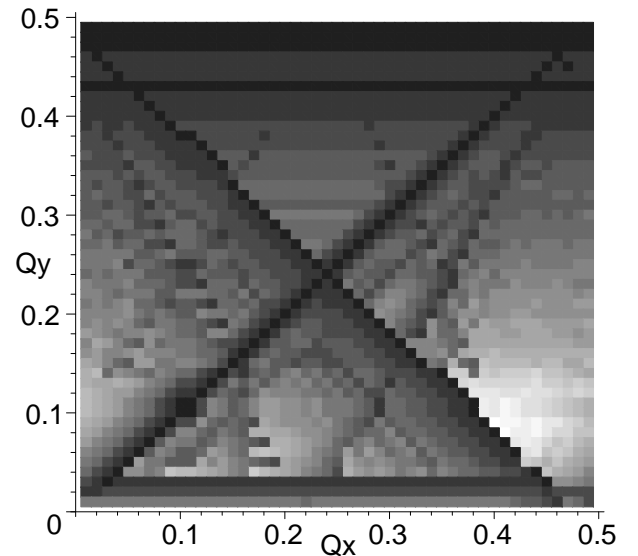


FIG. 10. $\delta = 0.01$, $\xi_{\max} = 0.200$. At each point in the tune plane the worst case from data such as that of Figs. 7 and 8 is picked and plotted, in this case with *strong* damping. Comparing with Fig. 9, note that the dependence on δ is weak over the entire tune plane.

VIII. COMPARISONS WITH EXISTING RINGS

Tune combinations for numerous existing colliding beam facilities are shown in Table III as well as in Fig. 5. Most of the entries in the table come from Rice [4]. The column labeled $\Delta Q_{y,\text{exp}}$ contains the experimentally determined quantity most directly comparable with theoretical value ξ_{th} . Though it is determined indirectly, $\Delta Q_{y,\text{exp}}$ is the vertical tune shift of a minimum amplitude particle, including the effect of the perturbation of the beta function at the crossing point due to the beam-beam force. The values ξ_{th} are determined by numerical iteration as explained in Sec. VII. In most cases the (minimal) Monte Carlo aspect of the procedure results in negligible fluctuation in ξ_{th} , exceptions are noted as footnotes. The significance of these fluctuations can also be assessed by the (relatively smooth) bin-to-bin transitions in resonance-free regions of the gray scale plots.

In constructing Table III, to account for multiple interaction points (IPs), the tunes and δ have been divided by the number of IPs, putting the calculation on a per IP basis. The measured LEP tune shifts, all with four IPs, fall far below the theoretical values, and a PEP-6IP point, not shown, shows even greater disagreement. Within the assumptions of the current model these points should agree, absent reasons that invalidate the comparison. But even small ring asymmetries invalidate the per-IP basis. Usually in rings with multiple IPs the optics of the various IPs are not identical and the phase advances between IPs are not constant; these effects invalidate the present theory. Furthermore,

since tune shifts from different IPs add directly, it is possible for the total tune shift in a ring with several IPs to approach 1/2 or even 1, and the implications of this have never been understood theoretically. Legitimate or not, the more-than-two-IP theory to experiment ratios have therefore been dropped from the averaging which then yields theory/experiment equal to 1.26 ± 0.45 . The one-IP average is 1.12 ± 0.43 .

It is difficult to draw conclusions from a survey such as this of beam-beam limit data from existing storage rings because the mixture of points from different storage rings does not indicate the huge variation of conditions, the time spent (possibly years) optimizing collisions and learning how to operate the collider, the level of imperfections present, the residual closed orbit, etc. These uncertainties can only reduce the level of agreement between theory and experiment.

IX. PREDICTIONS AND CONCLUSIONS

Predictions based on Eq. (41) for the performance of various proposed rings are shown in Table IV. The entries labeled CESR-1.9 are for the ‘‘CESRc’’ reconfiguration of CESR, currently in progress.

As expected there is extreme sensitivity to tunes, including synchrotron tune Q_s . For CESR-1.9 the very high proposed value $Q_s \approx 0.11$ appears to limit ξ_{th} seriously. Reducing Q_s (which is possible, at least in principle, for example, with a third harmonic cavity) gives a big improvement. Choosing optimal tunes is even more

TABLE III. Parameters of some circular, flat beam, e^+e^- colliding rings, and the saturation tune shift values predicted by Eq. (41). For points not excluded by one of these factors (see table footnotes) the mean and standard deviations of theory/experiment (the last column) are 1.26 ± 0.45 .

Ring	IPs	Q_x/IP	Q_y/IP	Q_s/IP	σ_s	β_y^*	$10^4 \delta_y$	ξ_{th}	$\Delta Q_{y,\text{exp}}$	$\xi_{\text{th}}/\Delta Q_{y,\text{exp}}$
VEPP4	1	8.55	9.57	0.024	0.06	0.12	1.68	0.028	0.046	0.61
PEP-1IP	1	21.296	18.205	0.024	0.021	0.05	6.86	0.076	0.049	1.55
PEP-2IP	2	5.303	9.1065	0.0175	0.020	0.14	4.08	0.050	0.054	0.93
CESR-4.7	2	4.697	4.682	0.049	0.020	0.03	0.38	0.037	0.018	2.06
CESR-5.0	2	4.697	4.682	0.049	0.021	0.03	0.46	0.034	0.022	1.55
CESR-5.3	2	4.697	4.682	0.049	0.023	0.03	0.55	0.029	0.025	1.16
CESR-5.5	2	4.697	4.682	0.049	0.024	0.03	0.61	0.027	0.027	1.00
CESR-2000	1	10.52	9.57	0.055	0.019	0.02	1.113	0.028	0.043	0.65
KEK-1IP	1	10.13	10.27	0.037	0.014	0.03	2.84	0.046	0.047	0.98
KEK-2IP	2	4.565	4.60	0.021	0.015	0.03	1.42	0.048	0.027	1.78
LEP-46	4 ^c	22.58	19.04	0.016	0.0076	0.05	0.958	0.128	0.034	
LEP-65	4 ^c	22.57	19.04	0.019	0.009	0.05	2.7	0.086		
LEP-98	4 ^c	24.59	24.05	0.029	0.0110	0.05	8.6	0.12 ^b	0.052	
PEP-LER	1	38.65	36.58	0.027	0.0123	0.0125	1.17	0.044	0.044	1.00
PEP-HER	1	24.57	23.64	0.045	0.0115	0.0125	1.98	0.056	0.026 ^a	
KEK-LER	1	45.518	44.096	0.021	0.0057	0.007	2.34	0.042	0.032	1.31
KEK-HER	1	44.525	42.135	0.019	0.055	0.007	2.18	0.060	0.018 ^a	
BEPC	1	5.80	6.70	0.020	0.05	0.05	0.16	0.068	0.039	1.74

^aIon effect blowup of low energy beam may prevent beam-beam saturation.

^bTheory value is erratic

^cUnequally spaced IPs.

TABLE IV. Parameters of some proposed rings and the saturation tune shift values predicted by Eq. (41). In all cases $\sigma_s = \beta_y^*$. The dependencies are far too complicated to be faithfully represented by such a limited set of data and small changes of tunes may yield substantially different values of ξ_{th} .

Ring	IPs	Q_x/IP	Q_y/IP	Q_s/IP	$10^4 \delta_y$	ξ_{th}
CESR-1.9	1	10.52	9.57	0.11	0.55	0.016 ^a
	1			0.03		0.026
	1	10.42	9.17	0.0		0.022
	1			0.11		0.030
	1			0.03		0.096
VLLC(e)	1	0.59	0.05	0.0	100	0.100
	1			0.11		0.044
	1	0.03	0.104			
VLHC(p)	1	0.59	0.05	0.0	10×10^{-8}	0.098
	1			0.03		0.056

^aTheory value is erratic.

important. In the full tune scans exhibited (as well as others not shown) the regions labeled “Good Region” in Fig. 5 appear to be more promising than other regions. And yet, at least as far as cases documented in Table III, these regions have never been tried operationally. Even within the present model there is resonant structure within these regions and effects not included, especially nonlinear resonances, would make it necessary to probe around for best operating points. For starters the fact that $Q_y = 0.67$ sits exactly on the third integer resonance would seem to contraindicate the upper two quadrants. But the so-called “good regions” are considerably larger than typical nonlinear stop bands, so the good regions in all four quadrants are candidates for good performance.

The location of good regions has been explained in this paper by the parametric resonator response illustrated in Fig. 4. Amplitude buildup occurs preferentially on the negative Q_x side of resonances [25]. Those resonances expected to be important in Table II are in fact visible in the tune plane plots, such as Fig. 8. Including synchrotron oscillations complicates the pattern considerably and favors low Q_s .

If one accepts the *saturation principle* and the numerical results of this paper there is potential for *large* increase in specific luminosity compared to existing operating points. Unfortunately, large specific luminosity does not guarantee large maximum luminosity, as nonlinear effects may limit the amount by which the beam currents can be increased above their threshold values. If the total beam current is limited, there may be favorable compromises, using more, but less intense, bunches, to exploit high specific luminosity.

For VLLC(e) (Very Large Lepton Collider) entries in Table IV, the tunes have arbitrarily been taken to be the same as for LEP-98 even though more favorable points exist (within the present model.) The achievable tune shift values are consistent with projections by Sen and Norem [26] and others, even though the extrapolation procedure

on which their values were based has been argued to be invalid.

The damping decrements δ of hadron colliders are some 10 orders of magnitude less than for electron machines. In spite of this big factor the maximum beam-beam tune shifts in proton machines are typically one-tenth of those in electron machines. For this reason, because δ has been thought to be important, it has usually been thought that entirely different mechanisms must be responsible for the limits. One effect contributing to the (relatively) large value ξ values achieved in proton machines is the fact that their beams are round rather than flat. But the (relatively) large ξ value achieved operationally with protons may also be partly explained by the relatively weak δ dependence claimed in the present paper. To pursue this line of reasoning, the bottom entry of Table IV shows the result of applying the formulas of this paper to the Very Large Hadron Collider VLHC(p). Comparing with the second VLLC(e) entry, changing the value of δ by 10 orders of magnitude alters ξ by only a factor of 0.54. This is consistent with a dependence $\xi \sim \delta^{0.06}$. Since this is not inconsistent with the dependence observed in electron machines (Fig. 2), it is possible that the physics of the beam-beam interaction may be much the same in proton as in electron colliding rings. If so, the luminosities of next-generation proton colliders may be much greater than current projections suggest. That said, the value $\xi_{th} = 0.056$ given in the table for VLHC(p) is undoubtedly too optimistic; other effects, such as diffusive beam growth, which will be strongly ameliorated by large δ , are likely to overwhelm the parametric pumping effect on which Table IV is based.

APPENDIX A: EXCITATION OF VERTICAL BETATRON MOTION BY AN EXTERNAL SHAKER

To illustrate the difference equation method it will be used in this section to calculate the vertical motion induced by the direct drive due to an external shaker. As well as

introducing the method of analysis, the equations of motion and an example of aliasing, this introduces the important damping decrement δ_y and shows how it influences the motion. (But the influence of δ_y on parametric drive need not be the same.)

The deflection caused by the external drive on the t th turn is

$$\Delta y'_t = F_E \cos \mu_E t. \quad (\text{A1})$$

We postulate a small ‘‘damping decrement’’ δ_y , so that the once-around transfer map in Twiss form is

$$\begin{pmatrix} y \\ y' - \Delta y'/2 \end{pmatrix}_{t+1} = \exp(-\delta_y) \begin{pmatrix} C_y + \alpha_y S_y & \beta_y S_y \\ \gamma_y S_y & C_y - \alpha_y S_y \end{pmatrix} \begin{pmatrix} y \\ y' + \Delta y'/2 \end{pmatrix}_t, \quad (\text{A2})$$

and a similar equation can be written for backwards propagation from t to $t - 1$. Note that y' is evaluated at the middle of the shaker. We are using the notation $C_y \equiv \cos \mu_y$ and $S_y \equiv \sin \mu_y$ and are intentionally using the subscript t as a turn index to be suggestive of the time measured in units of the revolution period. It will, however, always be an integer. Proceeding as in the derivation of Eq. (5) yields

$$y_{t+1} - 2C_y y_t + y_{t-1} = \beta_y S_y \Delta y'_t - \delta_y (y_{t+1} - y_{t-1}). \quad (\text{A3})$$

After solving this for y_t it will be possible to obtain y'_t from the equation

$$y'_t = \frac{y_{t+1} - y_{t-1} - 2\alpha_y S_y y_t + \delta_y (y_{t+1} + y_{t-1})}{2\beta_y S_y}. \quad (\text{A4})$$

As usual with driven oscillations we expect a response at the drive frequency, i.e.,

$$y_t = A \cos \mu_E t + B \sin \mu_E t, \quad (\text{A5})$$

where any transient [i.e., any solution of the homogeneous equation which is obtained by setting the drive term of Eq. (A3) to zero] has been neglected. In electron accelerators this neglect is justified by the existence of true damping. Even in proton accelerators where true damping is negligible, it can be justified by decoherence, or, as it is also called, Landau damping. Substituting into Eq. (A3) and equating the in-phase and the out-of-phase coefficients separately to zero, one obtains

$$A = \frac{\beta_y S_y (C_E - C_y)/2}{(C_E - C_y)^2 + \delta_y^2 S_E^2} F_E, \quad (\text{A6})$$

$$B = \frac{\beta_y S_y S_E \delta_y/2}{(C_E - C_y)^2 + \delta_y^2 S_E^2} F_E.$$

For near-resonance analysis we define [27,28]

$$\varepsilon = \mu_E - \mu_y. \quad (\text{A7})$$

Substituting into Eq. (A5) and neglecting terms containing $\varepsilon \delta_y$, we obtain

$$y_t = \frac{F_E \beta_y/2}{\varepsilon^2 + \delta_y^2} [-\varepsilon \cos \mu_E t + \delta_y \sin \mu_E t]$$

$$= -\frac{F_E \beta_y}{2\sqrt{\varepsilon^2 + \delta_y^2}} \cos(\mu_E t + \phi), \quad (\text{A8})$$

where $\phi = \tan^{-1}(\delta_y/\varepsilon)$, $\sin \phi = \delta_y/\sqrt{\varepsilon^2 + \delta_y^2}$, and $\cos \phi = \varepsilon/\sqrt{\varepsilon^2 + \delta_y^2}$. Taking $\alpha_y = 0$, the slope is given by

$$y'_t = \frac{F_E/2}{\varepsilon^2 + \delta_y^2} (\delta_y \cos \mu_E t + \varepsilon \sin \mu_E t)$$

$$= \frac{F_E}{2\sqrt{\varepsilon^2 + \delta_y^2}} \sin(\mu_E t + \phi). \quad (\text{A9})$$

These equations should be reminiscent of driven simple harmonic motion though they are the solution of the difference equations (A2). Except nearly on resonance, the in-phase $\cos \mu_E t$ term of Eq. (A8) is dominant, but for small ε , the out-of-phase $\sin \mu_E t$ dominates. The response always ‘‘lags,’’ with phase angle ϕ varying from zero to $-\pi$ as the drive frequency varies from zero to infinity. With $\phi = -\pi/2$ at resonance, the response changes sign in passing from below to above the resonance. The CS invariant of the motion is

$$\epsilon_{y,\text{CS}} = \frac{\beta_y F_E^2/4}{\varepsilon^2 + \delta_y^2}. \quad (\text{A10})$$

For small deflections the averaged change in $\epsilon_{y,\text{CS}}$ due to the shaker is

$$\langle \Delta \epsilon_{y,\text{CS}}^{(S)} \rangle \approx \langle 2y'_t \Delta y'_t \rangle$$

$$= \left\langle \frac{\beta_y F_E}{\varepsilon^2 + \delta_y^2} (\delta_y \cos \mu_E t + \varepsilon \sin \mu_E t) F_E \cos \mu_E t \right\rangle$$

$$= \frac{\beta_y F_E^2 \delta_y/2}{\varepsilon^2 + \delta_y^2}. \quad (\text{A11})$$

The averaged fractional change is therefore

$$\frac{\langle \Delta \epsilon_{y,\text{CS}}^{(S)} \rangle}{\epsilon_{y,\text{CS}}} = 2\delta_y. \quad (\text{A12})$$

This can be compared to the fractional change due to damping

$$\frac{\Delta \epsilon_{y,CS}^{(D)}}{\epsilon_{CS}} = -2\delta_y. \quad (\text{A13})$$

The fact that these changes are equal but opposite is consistent with the equilibrium.

APPENDIX B: HIGHER ORDER PARAMETRIC RESONANCES

From Eq. (A3) the equation of motion is

$$y_{t+1}(1 - \delta) - 2Cy_t + y_{t-1}(1 + \delta) = \beta S \Delta y'_t(x_t, y_t). \quad (\text{B1})$$

Here quantities without subscripts (β , μ , $C \equiv \cos\mu_y$, $S \equiv \sin\mu_y$ and δ) implicitly refer to y motion. Equation (14) was not the most general possibility for parametric resonance; let us seek a solution of the form [29,30]

$$y_t = \sum_m a_m \exp(im\tilde{\mu}t), \quad (\text{B2})$$

where $\tilde{\mu} = \mu + \varepsilon$ is close to μ in a sense to be spelled out below. The phase advance $\tilde{\mu}$ can be shifted by an integral multiple of 2π without altering Eq. (B2). Actually there is further degeneracy. The replacement $\mu \rightarrow \mu + \pi$ is equivalent to reversing the signs of both C and S . This reverses the signs of the y and y' outputs from the one-turn map around the storage ring. Since the deflection $\Delta y'_t$ is an odd function of y_t , the next beam-beam deflection is also reversed. This means that the replacement $\mu \rightarrow \mu + \pi$ is equivalent to toggling the sign of y_t every turn so the y axis points up for t even and down for t odd. The phase advance $\tilde{\mu}$ can therefore be shifted by $h\pi$ (h being an integer) without altering Eq. (B1). We therefore permit arbitrary half-integer additions to or subtractions from μ but require μ and $\tilde{\mu}$ to have the same fractional parts,

$$0 \leq \mu_{\text{frac}}, \quad \tilde{\mu}_{\text{frac}} < \pi, \quad \tilde{\mu} = \mu + \varepsilon, \\ \text{where } \tilde{\mu} - \tilde{\mu}_{\text{frac}} = \mu - \mu_{\text{frac}}. \quad (\text{B3})$$

Here the term ‘‘fractional’’ has been generalized to mean ‘‘modulo half-integers.’’ A resonance condition will presumably be met for ε sufficiently close to zero. This being a variation of constants method, the coefficients a_m are to be permitted to vary, but only *slowly* with time. Furthermore, since we are seeking normal modes of the system, they are assumed to have the common time dependence $\exp(i\omega t)$. Therefore, Eq. (B2) yields

$$y_{t+1} = \sum_m a_m (1 + i\omega) e^{im\tilde{\mu}} e^{im\tilde{\mu}t}, \\ y_{t-1} = \sum_m a_m (1 - i\omega) e^{-im\tilde{\mu}} e^{im\tilde{\mu}t}. \quad (\text{B4})$$

Suppressing the summation over n , Eq. (16) now takes the form

$$-\frac{\Delta y'_t}{4\pi\xi/\beta} \frac{2}{B_n} = \sum_m a_m \{ \exp[i(2n\mu_x + m\tilde{\mu})t] \\ + \exp[i(-2n\mu_x + m\tilde{\mu})t] \}. \quad (\text{B5})$$

Similar to μ , μ_x is subject to degeneracy; for arbitrary integer k , we define $0 \leq \mu_{x,\text{frac}} < \pi$ and permit $\mu_x = k\pi + \mu_{x,\text{frac}}$. Again the fractional parts are defined modulo half-integers. In this case the degeneracy is due to the fact that the deflection is an even function of x . When longitudinal motion is included there is a similar degeneracy in the choice of Q_s . In simulating performance I have simply taken Q_s to be fixed at a ‘‘small’’ value of order 0.1 or less [31]. The fractional ranges to be investigated are therefore

$$0 < Q_x < 0.5, \quad 0 < Q < 0.5, \quad Q_s = \text{fixed}. \quad (\text{B6})$$

The other three quadrants of modulo-integer fractional tunes will be identical. A resonance condition takes the form

$$2n\mu_x = \pm(2 + s)\tilde{\mu}, \\ \text{or, for } n \neq 0, \mu_x = \pm \frac{2 + s}{2n} (\mu + \varepsilon), \quad (\text{B7})$$

where s is a positive or negative integer. The integers h and k entering μ and μ_x to permit this condition to be satisfied are not, in general, the same. The tune degeneracies will be reflected by the fact that the coefficients in the equations are sinusoidal functions of the tunes and are therefore invariant to certain translations of the tunes. Also, there is other redundancy. For example, the replacement $s \rightarrow -4 - s$ has the same effect as an overall sign change.

It is these degeneracies (also known as aliasing) which make the spectrum of resonances ‘‘richer’’ than is the spectrum of resonances of the Mathieu equation. Any particular resonance can be identified by a (nonunique) combination of h, k, s, \pm . Even two different values of n can contribute to the same resonance, in which case two different values of B_n will enter the solution. The various ambiguities can, to some extent, be hidden, and a particular resonance isolated, by reexpressing the (externally controllable) parameter μ_x in terms of ε , as in the second of Eqs. (B7), allowing s to take all values except -2 (in which case there is no time varying parametric drive) and requiring $\varepsilon \ll 1$.

Using Eq. (B7) the right-hand side of Eq. (B1) can be manipulated into the form

$$-2\pi\xi SB_n \sum_m (a_{m-2-s} + a_{m+2+s}) \exp(im\tilde{\mu}t). \quad (\text{B8})$$

Substituting into Eq. (B1), dropping (small) terms containing $\omega\delta$, and setting the coefficients of $\exp(im\tilde{\mu}t)$ individually to zero yields, for $-\infty < m < \infty$,

$$\begin{aligned} & [(1+i\omega - \delta)e^{im\tilde{\mu}} - 2C + (1 - i\omega + \delta)e^{-im\tilde{\mu}}]a_m \\ & = -2\pi\xi SB_n(a_{m-2-s} + a_{m+2+s}). \end{aligned} \quad (\text{B9})$$

These equations reduce to

$$(\tilde{C}_m - C - \omega'\tilde{S}_m)a_m = -\pi\xi SB_n(a_{m-2-s} + a_{m+2+s}), \quad (\text{B10})$$

where some abbreviations have been introduced;

$$\begin{aligned} \omega' &\equiv \omega - i\delta, & \tilde{S}_j &\equiv \sin j\tilde{\mu} \equiv \sin j(\mu + \varepsilon), \\ \tilde{C}_j &\equiv \cos j\tilde{\mu} \equiv \cos j(\mu + \varepsilon). \end{aligned} \quad (\text{B11})$$

For any particular integer $s \neq 2$ and any positive integer n , Eq. (B10) forms an infinite set of equations, one for each integer m . To truncate this set we pick an arbitrarily large positive integer M and retain only the equations for $-M < m < M$ [32],

$$\begin{aligned} (\tilde{C}_M - C - \omega'\tilde{S}_M)a_M &= -\pi\xi SB_n(a_{M-2-s} + a_{M+2+s}), \\ (\tilde{C}_{M-1} - C - \omega'\tilde{S}_{M-1})a_{M-1} &= -\pi\xi SB_n(a_{M-3-s} + a_{M+1+s}), \\ &\dots \\ (\tilde{C}_1 - C - \omega'\tilde{S}_1)a_1 &= -\pi\xi SB_n(a_{-1-s} + a_{3+s}), \\ (1 - C)a_0 &= -\pi\xi SB_n(a_{-2-s} + a_{2+s}), \\ (\tilde{C}_1 - C + \omega'\tilde{S}_1)a_{-1} &= -\pi\xi SB_n(a_{-3-s} + a_{1+s}), \\ &\dots \\ (\tilde{C}_{M-1} - C + \omega'\tilde{S}_{M-1})a_{-M+1} &= -\pi\xi SB_n(a_{-M-1-s} + a_{-M+3+s}), \\ (\tilde{C}_M - C + \omega'\tilde{S}_M)a_{-M} &= \pi\xi SB_n(a_{-M-2-s} + A_{-M+2+s}). \end{aligned} \quad (\text{B12})$$

Coefficients with indices outside the range $-M < m < M$ are to be set to zero. Since these are linear, homogeneous equations, the solvability of the equations is governed by the determinant Δ of the matrix formed from their coefficients. Some properties of Δ can be obtained using a special case, $M = 2, s = 0$, as a model,

$$\Delta(\mu, \varepsilon, \omega'^2, \xi^2) = \det \begin{vmatrix} \tilde{C}_2 - C - \omega'\tilde{S}_2 & 0 & \pi\xi SB_n & 0 & 0 \\ 0 & \tilde{C}_1 - C - \omega'\tilde{S}_1 & 0 & \pi\xi SB_n & 0 \\ \pi\xi SB_n & 0 & 1 - C & 0 & \pi\xi SB_n \\ 0 & \pi\xi SB_n & 0 & \tilde{C}_1 - C + \omega'\tilde{S}_1 & 0 \\ 0 & 0 & \pi\xi SB_n & 0 & \tilde{C}_2 - C + \omega'\tilde{S}_2 \end{vmatrix}. \quad (\text{B13})$$

Since the a_0 equation does not depend on ω' , it can be solved for a_0 which can then be eliminated from the other equations. Reversing the sign of M obviously leaves the equations invariant, but the following observation is more essential: Just reversing the signs of the indices (e.g., $a_m \equiv b_{-m}$) cannot, on the one hand, alter the solvability of the equations, and, on the other hand, produces the same set of equations except with the sign of ω' reversed. It follows that the characteristic determinant is a function only of ω'^2 . That Δ depends only on ξ^2 can be inferred by multiplying both one row, for example, the second, and the corresponding column by -1 . This is equivalent to reversing the sign of ξ but leaving the equations and the determinant otherwise unaltered. Because Δ is a function only of $(\omega - i\delta)^2$, the substitution $\omega' = -i\delta$ yields $\Delta(\mu, \varepsilon, -\delta^2, \xi^2)$, a polynomial in δ^2 and ξ^2 with all coefficients real.

The simplest example of Eqs. (B12) has $s = 0$, $M = 1$. Dropping the $m = 0$ equation (because it does not contribute to lowest order) yields

$$\begin{aligned} (\tilde{C}_1 - C - \omega'\tilde{S}_1)a_1 &= -\xi S(a_{-1} + \hat{a}_3), \\ (\tilde{C}_{-1} - C - \omega'\tilde{S}_{-1})a_{-1} &= -\xi S(\hat{a}_{-3} + a_1). \end{aligned} \quad (\text{B14})$$

Terms to be dropped because they bring in coefficients outside the range being retained are indicated with circumflexes ($\hat{}$). (The rationale behind this approximation is that the retained terms a_1 and a_2 describe the dominant vertical motion, perturbed only in lowest order by the parametric pumping. Since neither of these coefficients appears in the $m = 0$ equation, that equation can be dropped—the error made is of higher order in the small parameter $\pi\xi SB_n$.) Continuing with the example, the condition to be satisfied for homogeneous Eqs. (B14) to have a nontrivial solution is

$$\det \begin{vmatrix} \tilde{C}_1 - C - \omega'\tilde{S}_1 & \xi S \\ \xi S & \tilde{C}_1 - C + \omega'\tilde{S}_1 \end{vmatrix} = 0. \quad (\text{B15})$$

From Eq. (B3) which defined ε , we can approximate $\tilde{C}_1 \approx C - \varepsilon S$, $\tilde{S}_1 \approx S$, to get

$$(\omega - i\delta)^2 = \varepsilon^2 - \xi^2. \quad (\text{B16})$$

This agrees with Eq. (23) and is even a slight improvement in that the damping has been handled explicitly and does not need to be inserted “by hand.” Expressed in terms of system parameters using Eqs. (B2) and (B7), the motion is stable if

$$\text{Re}\sqrt{\xi^2 - \left(\frac{2n\mu_x}{2+0} - \mu\right)^2} < \delta. \quad (\text{B17})$$

If $\delta = 0$ (no damping) the limits of the band of unstable motion are obtained more directly by setting $\omega' = 0$ in Eq. (B15),

$$\begin{vmatrix} \tilde{C}_1 - C & \xi S \\ \xi S & \tilde{C}_1 - C \end{vmatrix} = 0 \quad \text{or} \quad -\xi < \varepsilon < \xi. \quad (\text{B18})$$

$$\det \begin{vmatrix} (\tilde{C}_2 - C)/\tilde{S}_2 - \omega' & 0 & \xi S/\tilde{S}_2 & 0 \\ 0 & (\tilde{C}_1 - C)/\tilde{S}_1 - \omega' & 0 & \xi S/\tilde{S}_1 \\ -\xi S/\tilde{S}_1 & 0 & -(\tilde{C}_1 - C)/\tilde{S}_1 - \omega' & 0 \\ 0 & -\xi S/\tilde{S}_2 & 0 & -(\tilde{C}_2 - C)/\tilde{S}_2 - \omega' \end{vmatrix} = 0. \quad (\text{B19})$$

The four solutions of this equation for ω' are the exponents of the possible homogeneous motions of the system. The elements of this matrix have been obtained by reading coefficients directly from Eq. (B12). For fixed n , s , and μ , since $\tilde{\mu} = 2n\mu_x/(1+s)$, each of these eigenvalues is a function of μ_x and ξ_n . Unstable regions of the (μ_x, ξ_n) parameter space are characterized by at least one of these eigenvalues having a positive real part.

Since instability boundaries are marked by the vanishing of Δ for $\omega = 0$, we will be interested primarily in the case of small ξ and δ . We therefore define an expansion [33]

$$\begin{aligned} \Delta(\mu, \varepsilon, -\delta^2, \xi^2) &= \Delta_{00}(\mu, \varepsilon) + \Delta_{10}(\mu, \varepsilon)\xi^2 \\ &+ \Delta_{01}(\mu, \varepsilon)\delta^2 + \Delta_{11}(\mu, \varepsilon)\xi^2\delta^2 \\ &+ \dots \end{aligned} \quad (\text{B20})$$

This series terminates; the termination depends on M , which is fixed. Because of the aliasing discussed previously, Eq. (B20) has a very complicated global dependence on ε . To help in identifying local resonances, and because we cannot simply set $\varepsilon = 0$, we must also expand for small ε ,

To obtain a more accurate formula (for the same $s = 0$ resonance) one must retain more terms. [For this case the determinant needed for the next approximation was already exhibited in Eq. (B13).] In general, after eliminating a_0 , there are $2M$ equations in $2M$ unknowns. For fixed n , s , and μ , the determinant is a function of ε and ξ . The vanishing of the determinant formed from the coefficients determines the stability boundaries in the (ε, ξ) parameter space.

The stability of motion can be formulated in terms of the eigenvalues of a matrix. To illustrate this, and to exhibit a different resonance, consider the case $s = 1$, $M = 2$. In this case the central equation can be dropped (to lowest order) since it does not couple a_0 to any of the retained coefficients. Solvability requires the vanishing of the determinant

$$\begin{aligned} \Delta(\mu, \varepsilon, -\delta^2, \xi^2) &= \Delta_{100}(\mu)\xi^2 + \Delta_{010}(\mu)\delta^2 \\ &+ \Delta_{110}(\mu)\xi^2\delta^2 + \dots \\ &+ \Delta_{101}(\mu)\xi^2\varepsilon + \Delta_{011}(\mu)\delta^2\varepsilon \\ &+ \Delta_{111}(\mu)\xi^2\delta^2\varepsilon + \dots + \Delta_{002}(\mu)\varepsilon^2 \\ &+ \Delta_{102}(\mu)\xi^2\varepsilon^2 + \Delta_{012}(\mu)\delta^2\varepsilon^2 \\ &+ \Delta_{112}(\mu)\xi^2\delta^2\varepsilon^2 + \dots \end{aligned} \quad (\text{B21})$$

There is no leading term $\Delta_{000}(\mu, \varepsilon)$ since that term corresponds to the absence of perturbation. The coefficient $\Delta_{001}(\mu, \varepsilon)$ also vanishes since, in the no perturbation limit, Δ is an even function of ε . The Δ 's are trigonometric polynomials of μ . The very complicated dependencies of the coefficients on μ will (presumably) cause the resonance strengths to exhibit erratic global variation.

This complication can be hidden formally by treating the Δ_{ijk} coefficients as constants, i.e., by holding μ fixed. For example, as ξ increases from zero, with ε sufficiently small, a nearby instability boundary is encountered for

$$\xi^2 = \frac{-\Delta_{002}\varepsilon^2 + \Delta_{010}\delta^2 + (\Delta_{011}\varepsilon + \Delta_{012}\varepsilon^2)\delta^2}{\Delta_{100} + \Delta_{101}\varepsilon + \Delta_{110}\delta^2 + \Delta_{102}\varepsilon^2 + (\Delta_{111}\varepsilon + \Delta_{112}\varepsilon^2)\delta^2}. \quad (\text{B22})$$

The leading part of the denominator, $\Delta_{100} + \Delta_{101}\varepsilon$, is either negative or can be made negative by choosing the appropriate sign for ε , then the overall expression is positive (for sufficiently small δ) in those cases for which $\Delta_{002} > 0$. This makes ξ real, which implies true resonance, at least in this case, and there are other possibilities.

To study the resonances in greater detail it is appropriate to proceed in close analogy with traditional treatments of the Mathieu equation. That is, holding μ and δ fixed, let us plot ε as a function of ξ for the curve or curves separating stable and unstable regions, as they emanate from the origin ($\xi = \varepsilon = 0$). For this purpose an expansion

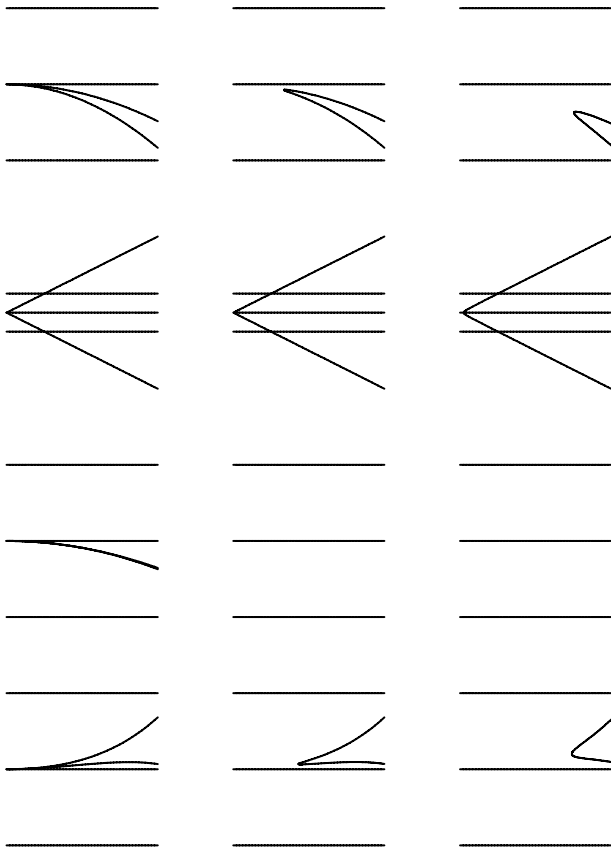


FIG. 11. $\varepsilon_{\pm}(0)$, $\varepsilon_{\pm}(1/1000)$, $\varepsilon_{\pm}(1/200)$. The edges of instability bands are plotted on the range $0 < \xi < 0.2$, where ξ is the abscissa and ε is the ordinate. Vertically arrayed, starting at the top, the plots correspond to $s = -1, 0, 1, 2$ with $M = s + 1$. Horizontally arrayed, the damping decrements are $\delta = 0, 1/1000, 1/200$, as indicated in parenthesis. The vertical phase advance for this plot is $\mu_y = 0.57 \times 2\pi$. Horizontal lines mark $\varepsilon = -0.05, 0, 0.05$. For the dominant $s = 0$ resonance (second from top) the displacement of the threshold away from $\xi = 0$ is just barely visible for $\delta = 1/200$ and the stop band width is proportional to ξ , as is true for the Mathieu equation. For higher order stop bands the threshold dependence on δ is much stronger and the power of the power law dependence increases as the order increases. These features are also exhibited by the Mathieu equation with damping.

more compact than Eq. (B21) is (suppressing μ and δ arguments)

$$\Delta_{\mu,\delta}(\varepsilon, \xi) = \Gamma_0(\xi) + \Gamma_1(\xi)\varepsilon + \Gamma_2(\xi)\varepsilon^2 + \dots \quad (\text{B23})$$

These coefficients $\Gamma_i(\xi)$ are obtained simply from the $\Delta_{ijk}(\mu)$ coefficients defined previously. Setting $\Delta = 0$ and solving Eq. (B23) (keeping only the terms shown) yields

$$\varepsilon_{\mu,\delta}(\xi) = \frac{-\Gamma_1(\xi) \pm \sqrt{\Gamma_1^2(\xi) - 4\Gamma_2(\xi)\Gamma_0(\xi)}}{2\Gamma_2(\xi)}. \quad (\text{B24})$$

The dependence of these roots $\varepsilon_{\mu,\delta,\pm}$ on ξ for particular values of δ and μ are plotted in Fig. 11. Values of ξ for

which the roots are complex do not show up on these plots. This plot is strikingly similar to the plot of the instability boundaries of the Mathieu equation [12].

The threshold value ξ_{thr} satisfies

$$\Gamma_1^2(\xi_{\text{thr}}) - 4\Gamma_2(\xi_{\text{thr}})\Gamma_0(\xi_{\text{thr}}) = 0. \quad (\text{B25})$$

- [1] J. Seeman, in *Nonlinear Dynamics Aspects of Particle Accelerators*, Lecture Notes in Physics Vol. 247 (Springer-Verlag, New York, 1985), p. 121.
- [2] D. Brandt *et al.*, Rep. Prog. Phys. **63**, 939 (2000).
- [3] E. Keil and R. Talman, Part. Accel. **14**, 109 (1983).
- [4] D. Rice, Laboratory of Nuclear Studies, Cornell University Report No. CBN 01-09, 2001 (unpublished); CESRc PAC report, 2001(unpublished); (private communication).
- [5] It is not quite accurate to say that the horizontal treatment is weak-weak since, in fact, the horizontal beam-beam tune is allowed to shift arbitrarily, proportional to beam current and hence also proportional to the vertical tune shift, until the latter saturates. Presumably the main effect of horizontal tune shift is to increase the spread of horizontal tunes and hence to increase the number of resonants effective. But otherwise the horizontal treatment is weak-weak.
- [6] S. Myers, ERN LEP Note No. 362, 1982; S. Peggs and R. Talman, Phys. Rev. D **24**, 239 (1981).
- [7] J. Tennyson, in *Physics of High Energy Particle Accelerators*, edited by R. Carrigan, F. Huson, and M. Month, AIP Conf. Proc. No. 87 (AIP, New York, 1982), p. 35.
- [8] J. Tennyson, SLAC-PUB-2624, CONF-80051021 (1980).
- [9] The assumption of negligible beam height uses the result that synchrotron-radiated photons are emitted precisely in the forward direction; since their typical angle is $1/\gamma$ this is an excellent, but not perfect assumption.
- [10] The instability to be described causes nondestructive growth to a well-defined amplitude, *not* unlimited exponential growth. Therefore the term “barely stable” in the saturation principle could more accurately be replaced by “barely unstable at zero amplitude.” In the picture being promoted, most of the particles are oscillating more or less stably (with random, uniformly distributed, phases) at the amplitudes to which they have been pumped. The amplitude of any particle that “loses lock” from its own pumping decays toward zero until the particle gets caught up again.
- [11] Lord Rayleigh, *Scientific Papers* (Cambridge University Press, Cambridge, 1900), Vol. I, p. 97; Lord Rayleigh, *Scientific Papers* (Cambridge University Press, Cambridge, 1900), Vol. II, p. 1 (1900) (Dover reprint 1964).
- [12] N. McLachlan, *Theory and Application of Mathieu Functions* (Dover, New York, 1964).
- [13] L. Landau and E. Lifshitz, *Mechanics* (Butterworth-Heinemann, Oxford, 1976), p. 80.
- [14] *Basic Theory of Oscillations*, edited by V. Migulin (Mir Publishers, Moscow, 1983).
- [15] From this point forward in this paper quantities without subscripts, such as ξ , β , Q , and σ , will implicitly refer to y motion. The one exception, to avoid a clash of symbols later on, will be a_y .

- [16] The beam-beam deflection also depends on horizontal position x and longitudinal position s ; these dependencies will be incorporated later.
- [17] Tunes Q and phase advances per turn $\mu = 2\pi Q$ will be interchanged as convenient, and without warning, and either may be referred to as a frequency.
- [18] The fact that Eq. (5) generalizes the Mathieu equation can be seen by re-expressing it as $(y_{t-1} + y_{t+1} - 2y_t) + \delta(y_{t+1} - y_{t-1}) + 2(1 - C_y)y_t + \beta S_0 \Delta y'(t) = 0$. In the so-called smooth approximation (fractional changes per turn assumed small), the first term reduces to \ddot{y} , and the second to $2\delta\dot{y}$, the damping term in simple harmonic motion. The term $2(1 - C_y)y_t$ generalizes the restoring force term. The term $\beta S_0 \Delta y'$, proportional to y_t for small y_t , makes the system nonautonomous through its dependence on x_t and s_t , and provides the parametric drive.
- [19] The dependence on amplitude a has been incorporated into the *ad hoc* factor $[1 - \exp(-a^2/\sigma^2)]$ in Eq. (8) to recover the correct tune shift at large a while retaining the leading ($\sim a^2$) behavior.
- [20] The longitudinal factor in Eq. (11) results from the dependencies: beam height $\sim \sqrt{\beta_y(s)}$, tune shift $\sim \beta_y(s) \times$ charge density, and $\beta_y(s)/\beta_y(0) = 1 + [s/\beta_y(0)]^2$. A strictly faithful treatment would convolve the square root factor in Eq. (11) with the longitudinal density distribution, but this has not been done.
- [21] In the jargon of ordinary differential equations, introducing the Fourier series of Eq. (12) converts a Mathieu equation into a Hill equation [12].
- [22] G. N. A. Watson, *Bessel Functions* (Cambridge University Press, Cambridge, 1966), 2nd ed.
- [23] The stability limits (24) (though not the growth rate in the interior) could have been determined by setting $\dot{a} = \dot{b} = 0$ in Eq. (21). The justification is that the amplitude neither grows nor shrinks at the ends of the stop band.
- [24] The effect of dependence of μ_s on a_s has not been investigated.
- [25] For same-sign colliders $\xi < 0$ and the negative- Q_x side is the “good side” of resonances. This has been confirmed numerically.
- [26] T. Sen and J. Norem, Phys. Rev. ST Accel. Beams **5**, 031001 (2002).
- [27] It is the equality of cosines, rather than the equality of tunes, that causes resonance. To handle this all tunes can be aliased into fractional tunes in a range from 0 to 0.5. This effectively reduces the resonance-free fractional tune landscape by a factor of 2.
- [28] Note the distinction between the symbol ε for frequency deviations and the symbol ϵ for Courant-Snyder invariants.
- [29] Unless otherwise noted, summations over m run over all integers from $-\infty$ to ∞ .
- [30] Ordinarily an *ansatz* such as Eq. (B2) would be made in preparation for finding nonlinear harmonics, intending to truncate higher Fourier terms. Here, because the drive is parametric, the equations will remain linear. There will be a certain amount of “leakage” if the series is truncated, but this is mainly a question of convenience, and there is no possibility of the chaotic motion that characterizes nonlinear equations. This may be somewhat academic as the growth the equations exhibit can lead to amplitudes for which nonlinearity becomes important and the linearity assumption loses validity.
- [31] Though the synchrotron and horizontal oscillation frequencies are certain to be incommensurate in practice, without care they are likely to be commensurate in a simulation in which both values are “put in by hand.” This could lead to unphysical resonant artifacts.
- [32] For a parametrically driven mechanical system, described by a nonautonomous differential equation such as the Mathieu equation or the Hill equation, Eqs. (B12) would be known as “Hill equations.”
- [33] For convenience in all subsequent formulas we set $\pi B_n = 1$. This is equivalent to having redefined ξ so the factors can be restored by the replacement $\xi \rightarrow \pi B_n \xi$. As it happens, 1 is a typical value for πB_n .